Computers and Operations Research 84 (2017) 127–145

Contents lists available at ScienceDirect

Computers and Operations Research

journal homepage: www.elsevier.com/locate/cor

Integrated aircraft-path assignment and robust schedule design with cruise speed control

Özge Şafak[a], Sinan Gürel[b], M. Selim Aktürk[a,*]

[a] Department of Industrial Engineering, Bilkent University, 06800 Bilkent, Ankara, Turkey
[b] Department of Industrial Engineering, Middle East Technical University, Ankara 06800, Turkey

ARTICLE INFO

Article history:
Received 25 October 2015
Revised 11 March 2017
Accepted 12 March 2017
Available online 22 March 2017

Keywords:
Fleet type assignment
Airline scheduling
Cruise time controllability
Second order conic programming
Chance constraints

ABSTRACT

Assignment of aircraft types, each having different seat capacity, operational expenses and availabilities, critically affects airlines' overall cost. In this paper, we assign fleet types to paths by considering not only flight timing and passenger demand, as commonly done in the literature, but also operational expenses, such as fuel burn and carbon emission costs associated with adjusting the cruise speed to ensure the passenger connections. In response to flight time uncertainty due to the airport congestions, we allow minor adjustments on the flight departure times in addition to cruise speed control, thereby satisfying the passenger connections at a desired service level. We model the uncertainty in flight duration via a random variable arising in chance constraints to ensure the passenger connections. Nonlinear fuel and carbon emission cost functions, chance constraints and binary aircraft assignment decisions make the problem significantly more difficult. To handle them, we use mixed-integer second order cone programming. We compare the performance of a schedule generated by the proposed model to the published schedule for a major U.S. airline. On the average, there exists a 20% overall operational cost saving compared to the published schedule. To solve the large scale problems in a reasonable time, we also develop a two-stage algorithm, which decomposes the problem into planning stages such as aircraft-path assignment and robust schedule generation, and then solves them sequentially.

1. Introduction

To achieve significant cost savings for the airline industry, the fuel cost, which has the major component of overall operational expenses, should be considered in the airline scheduling process. In general, fuel expenses account for about 30% of total operating cost. However, in 2008, the share for fuel costs rose to 50% with the sharp increase in the fuel prices (ICAO, 2009). In addition to rising fuel costs, greenhouse gas emissions are becoming significantly more important for airlines, as climate change is becoming an ever more important subject in the world. Aviation was the first sector to agree upon ambitious targets. One of the targets is a 50% reduction in net aviation CO_2 emissions by 2050 compared to 2005 levels (IATA, 2013). Airlines have committed to achieve these through improved engine technologies, infrastructure improvement and better operations. As discussed in Marais and Waitz (2009), fuel consumption per passenger kilometer has decreased by 70% over the past four decades. In response to fuel expenses and emission restrictions, in this paper, we manage airline operations efficiently, such as flight re-timing and fleet assignment to minimize the fuel burn and CO_2 emission costs by incorporating cruise speed control to ensure passenger connections.

Assignment of aircraft types, each having different seat capacity, operational expenses and availabilities, has a significant impact on the airlines' overall cost. In this paper, we assign fleet types by considering not only flight timing and passenger demand, as commonly done in the literature, but also operational expenses, such as fuel burn and carbon emission costs. We generate a robust schedule with improved capability in response to flight time uncertainty due to airport congestions. We simultaneously re-time the flight departure times and control the cruise speed to ensure the passenger connections at a desired service level. We provide more slack over vulnerable connections at the congested airports and remove excess slack from the remaining connections. We can increase the connection possibilities by increasing the cruise speed and inserting idle times. However, this strategy incurs additional cost of idle times and costs of fuel and carbon emissions associated with speed adjustment. An important question arises as to whether one could improve the solution through assigning a fuel efficient aircraft to an aircraft path with a high variability, which also has connected passengers. If a fuel efficient but smaller aircraft is assigned to

* Corresponding author.
E-mail address: akturk@bilkent.edu.tr (M.S. Aktürk).

http://dx.doi.org/10.1016/j.cor.2017.03.005
0305-0548/

a flight, some of the passengers may not be accommodated due to the limited seat capacity and be turned away by the airline, thus resulting in high passenger spill costs. If a larger aircraft with higher seat capacity is assigned to the same flight, passenger demand could be met but this directly increases the flight operating costs such as fuel and emission costs. Therefore, there is a need to consider all of these interrelated cost terms simultaneously to minimize the overall operating cost of the entire flight network.

Hai and Barnhart (2013) has introduced a dynamic airline scheduling approach that changes the schedule slightly by re-timing and re-fleeting during the booking period. To reflect changing demand, re-timing allows the flight departure times slightly vary within specified time intervals to increase the passenger connection opportunities and a more cost effective fleeting possibility. Based on the updated passenger demand during the booking period, re-fleeting adjusts the capacity by re-assigning aircraft types to flight legs to reduce the operational costs and increase the passenger revenues. Sherali et al. (2005) propose a demand-driven refleeting model that dynamically reassigns aircraft based on the improved demand forecasts so as to maximize the total revenue. In order to preserve the crew assignment, the aircraft reassignment is limited within the same aircraft family. To deal with highly uncertain demand well in advance in departures, Sherali and Zhu (2008) propose a two-stage stochastic mixed integer programming approach. In the first stage, they only assign aircraft families to each flight leg. After receiving the improved demand forecasts, refleeting process within each family is conducted for each forecasted demand realization in the second stage. Jarrah et al. (2000) also present a refleeting model while limiting the number of changes to the original fleet assignment. In the re-fleeting approach, they re-assign the fleet types to scheduled flight legs with minor adjustments. They only allow the swapping aircraft within the same aircraft family or put restrictions on the changes to the original schedule, because airlines wish to preserve the crew schedules which have to be constructed one or two months prior to flight departures due to the crew regulations. Similarly, in our proposed study, we wish to leave the aircraft paths unchanged in order to eliminate additional costs of adjustment. We assign aircraft types to these paths.

Rexing et al. (2000) model the basic fleet assignment problem with time windows in order to improve the fleet assignment solutions. Mercier and Soumis (2007) show that allowing changes on the scheduled departure times within an integrated aircraft routing and crew scheduling model yields significant cost savings. Papadakos (2009) also includes re-timing possibilities for aircraft routing and crew scheduling. Sherali et al. (2013) propose a model that integrates the schedule design and fleet assignment while allowing flight departure times vary within time windows. They claim that retiming approach increases the connection opportunities for passengers and generates more profitable schedules. In general, the flexibility in departure times is achieved with multiple discretized copies of the flight legs within specified time intervals. As opposed to discrete time units, in our proposed study, we allow the departure time of each flight continuously vary within a given time interval. In addition to flexible departure times, we control the cruise times to provide more opportunity to satisfy the passenger connections.

When planned schedule is disrupted, aircraft routings, crew pairings and passenger itineraries have to be recovered. Traditional airline recovery approaches ignore passenger itineraries until the end of the recovery process so recovered schedule may not be feasible for passenger flow. Maher (2015) considers the passenger flows in integrated schedule, aircraft and crew recovery problems. Burke et al. (2010) observe the effect of a randomly generated disruption on KLM airlines' schedule. They obtain recovery by simultaneous flight retiming and aircraft rerouting.

Most scheduling models ignore the unexpected flight delays to limit the complexity. However, flight delays may result in disruption on the passenger and aircraft connections, thereby lead to loss of time and customer goodwill. This is the reason why many airlines have been recently interested in generating a robust schedule with improved capability in response to variability in airline operations. Weide et al. (2010) produce solutions that are robust to variability in airline operations for aircraft routing and crew pairing problem by penalizing aircraft changes under short connection times. A common approach in coping with delays is to leave idle times. Ahmadbeygi et al. (2010) and Chiraphadhanakul and Barnhart (2013) propose models minimizing delay propagation in entire network by redistributing the existing slack. They adjust flight departure times to provide more slack over critical connections and draw excess slack from others. Lan et al. (2006) propose a mixed integer programming model, which minimizes the delay propagation by allowing changes in aircraft assignment, and develop an approach to reduce the passenger misconnections by re-timing the flight departure times for a fixed fleet assignment. More recently, Dunbar et al. (2014) incorporate delay scenarios within the aircraft routing and crew pairing problems while re-timing of flight departures. In a similar way, they use re-timing approach to provide slack across the connections so as to minimize delay propagation. To capture the uncertainties in flight block times, Arıkan and Deshpande (2012) model the flight block time distribution and provide a method for estimating the schedule on-time arrival probability. Sohoni et al. (2011) propose models that capture uncertainties related with block time through chance constraints and consider flight re-timing. The aim is to maximize expected profit while improving on-time performance measure and passengers' service level. Duran et al. (2015) design a robust flight schedule incorporating cruise time controllability. They propose a model which captures the variability in flight duration due to the airport congestions via a random variable representing noncruise times.

In the existing literature, cruise time has been often taken as a fixed parameter, although there occur options of flying faster to increase passenger connection possibilities and flying slower for conservation of fuel as discussed in Cook et al. (2009). Bertsimas et al. (2010) decide on an optimum combination of flow management actions, including ground holding, rerouting, speed control and airborne holding. They control the speed through adjustments in the time spent in each en route sector. However, they do not consider fuel burn and carbon emission costs associated with speed adjustment. Sherali et al. (2006) state that airline optimization models are quite sensitive to fuel burn. Tetzloff and Crossley (2010) address environmental and economic considerations by developing a model determining the new and existing aircraft assignment such that all passenger demand is met. The major difficulty of incorporating cruise speed control is that the fuel burn and carbon emission cost functions are nonlinear functions of cruise speed. Consequently, handling the nonlinear model in a reasonable amount of time is critical for solving such problems. To overcome this difficulty, we use mixed integer second order cone programming as discussed in Aktürk et al. (2014).

The contributions of this paper include the following:

- We consider the fuel burn and CO_2 emissions costs associated with adjusting cruise speed to ensure the passenger connections. Therefore, we may prefer to assign a fuel efficient but smaller aircraft to an aircraft path involving critical passenger connections in albeit of an additional cost of spilled passengers.
- We assign fleet types by considering not only flight timing and passenger demand, as commonly done in the literature, but also operational expenses, such as fuel burn and carbon emission costs.

- The proposed model has nonlinear fuel and emission cost terms and chance constraints to ensure the passenger connections with a desired probability. To handle nonlinearity, we utilize mixed integer second order cone programming (MISOCP).
- We devise a two-stage algorithm, which decomposes the problem into two planning stages such as aircraft-path assignment and robust schedule design, and then solves them sequentially.
- We present extensive computational results using a schedule for a major U.S. airline to demonstrate the high quality performance of the two-stage algorithm.

We organize the remainder of this paper as follows. In Section 2, the framework of the problem is briefly described. A proposed mathematical model is given with a numerical example. Section 3 is devoted to the conic reformulation of the proposed model in detail. We describe our approach to simplify the problem and two-stage algorithm in Section 4. We report the computational results in Section 5. Finally, in Section 6, we conclude with remarks and outline possible research directions arising from this study.

2. Problem definition

In this study, we would like to assign fleet types to given flight paths during the booking period. We consider not only flight timing and passenger demand, as commonly done in the literature, but also operational expenses, such as fuel burn and carbon emission costs associated with cruise speed adjustment to ensure the passenger connections. Therefore, we propose a bi-criteria optimization model. The first objective is to reduce the airline overall operational cost, where as the second objective is to increase the passenger connection probabilities under the non-cruise time uncertainties due to the airport congestions. We satisfy passenger connections in the entire network through the chance constraints. To achieve desirable connection probabilities, we allow minor adjustments on the flight departure times by redistributing the existing slack over vulnerable connections and removing excess slack from the remaining connections. Simultaneously, we control the cruise speed to ensure desirable connection probabilities. However, there occur additional fuel and CO_2 emission costs associated with speed adjustment. In order to reduce the fuel expenses, one approach is to assign a fuel efficient aircraft to an aircraft path with critical passenger connections. On the other hand, fuel efficient but a smaller aircraft may cause an additional cost of spilled passengers or lost revenue due to under-capacity. In this study, our main claim is that we may compensate the cost of spilled passengers by assigning fuel efficient aircraft, when we consider the fuel burn and CO_2 emissions costs associated with adjusting cruise speed to ensure the passenger connections.

In the booking period, airlines wish to keep generated schedule close to the original one designed well in advance. Because, even minor changes on flight schedule or aircraft routes may lead to a massive disruption on the aircraft, passenger and crew connections. Therefore, we work with all aircraft paths which have been determined through the airlines' scheduling choices. We define an aircraft path to be a sequence of flights operated by an individual aircraft in a given time period. All input paths form a complete partition of all the flights.

The notation used throughout the paper is given below:

Parameters

T	set of aircraft types
P	set of paths
J	set of flights
J_p	set of flights in path $p \in P$
N^t	available number of aircraft of type $t \in T$
CAP^t	number of seats in aircraft of type $t \in T$
$[f_i^{t,l}, f_i^{t,u}]$	time window for cruise time of flight $i \in J$ with aircraft $t \in T$
A_i	random variable representing the non cruise time of flight $i \in J$
$E[A_i]$	expected non-cruise time of flight $i \in J$
$PAIR$	set of pairs of consecutive flights of the same aircraft
TA_{ij}^t	turnaround time needed to prepare aircraft $t \in T$ between flights $i, j \in PAIR$
D_i	number of passenger demand of each flight $i \in J$
Csp_i	cost of spilled passengers of flight $i \in J$
c_{fuel}	cost of fuel per kg of aircraft fuel consumption
c_{CO_2}	cost of emission per kg of aircraft CO_2 emission
I^t	unit idle time cost of aircraft of type $t \in T$ in dollars per minute
P_i	set of flights that have a passenger connection with flight $i \in J$
TP_{ij}	turntime needed to connect passengers between flights $i \in J, j \in P_i$
γ_{ij}^d	minimum service level for each passenger connection between flights $i \in J$ and $j \in P_i$
w_{ij}	weight of the passenger connection between flights $i \in J, j \in P_i$
$[v_i^l, v_i^u]$	time window for the departure time of flight $i \in J$
O_i	origin of flight $i \in J$
Dn_i	destination of flight $i \in J$
B	set of airports
e_b	airport congestion coefficient for airport $b \in B$

Decision Variables

z_p^t	1 if aircraft of type $t \in T$ is assigned to path $p \in P$, and 0, otherwise.
x_i	departure time of flight $i \in J$
f_i^t	cruise time of flight $i \in J$ with aircraft type $t \in T$
S_i^t	idle time of flight $i \in J$ with aircraft type $t \in T$
γ_{ij}	service level for passenger connections between flights $i \in J$ and $j \in P_i$, i.e., probability that passengers from flight i can connect to any follow-on flight $j \in P_i$

2.1. Mathematical model

The proposed nonlinear mathematical model is provided below.

$$\min \quad F1: \quad \sum_{p\in P}\sum_{i\in J_p}\sum_{t\in T} C_{fuel\&CO_2}^{i,t}(f_i^t) + \sum_{p\in P}\sum_{i\in J_p}\sum_{t\in T} Csp_i \cdot max\left(D_i - CAP^t, 0\right)\cdot z_p^t + \sum_{i\in J}\sum_{t\in T} S_i^t \cdot I^t \tag{1}$$

$$\max \quad F2: \quad \sum_{i\in J}\sum_{j\in P_i} w_{ij}\cdot\gamma_{ij} \tag{2}$$

subject to

$$\sum_{t\in T} z_p^t = 1 \qquad p \in P \tag{3}$$

$$\sum_{p\in P} z_p^t \le N^t \qquad t \in T \tag{4}$$

$$Pr\left[A_i + \sum_{t\in T} f_i^t \le x_j - x_i - TP_{ij}\right] \ge \gamma_{ij} \qquad i \in J, j \in P_i \tag{5}$$

$$\gamma_{ij} \geq \gamma_{ij}^{d} \qquad i \in J, j \in P_i \tag{6}$$

$$f_i^{t,l} \cdot z_p^t \leq f_i^t \leq f_i^{t,u} \cdot z_p^t \qquad p \in P, i \in J_p, t \in T \tag{7}$$

$$x_j - x_i - \sum_{t \in T} TA_{ij}^t \cdot z_p^t - \sum_{t \in T} f_i^t - E[A_i] - \sum_{t \in T} S_i^t = 0 \quad (i,j) \in PAIR \tag{8}$$

$$v_i^l \leq x_i \leq v_i^u \qquad i \in J \tag{9}$$

$$w_i^l \leq x_i + \sum_{t \in T} f_i^t + E[A_i] \leq w_i^u \qquad i \in J \tag{10}$$

$$S_i^t \leq M \cdot z_p^t \qquad p \in P, i \in J_p, t \in T \tag{11}$$

$$S_i^t \geq 0 \qquad i \in J, t \in T \tag{12}$$

$$z_p^t \in \{0,1\} \qquad p \in P, t \in T \tag{13}$$

The most common objective that airlines minimize is the overall operational cost. However, a schedule that minimizes the operational cost may not ensure a high service level for passengers' connections. Thus, in this study, we consider a bi-criteria problem. The first objective minimizes the overall operational cost and the second objective maximizes the overall service level for passenger connections through the entire network. The sum of fuel cost, CO_2 emission cost, spilled passengers cost and idle time cost over all flights in the network constitute airline's operational cost. Moreover, overall service level for passenger connections is the weighted average of the service level for each passenger connection in the network. Constraint (3) guarantees that each path is assigned to exactly one aircraft type. Constraint (4) limits the number of employed aircraft by N^t. Constraint (5) is a chance constraint to ensure each passenger connection with a desirable service level. We require the probability that passengers from flight i can connect to any follow-on flight $j \in P_i$, to be greater than or equal to service level variable γ_{ij}. Constraint (6) applies a desired lower bound on the service level variable γ_{ij}. Constraint (7) applies cruise time upper and lower bound for each flight. Constraint (8) guarantees minimum aircraft turnaround time between two consecutive flights. In (9) and (10), we want the departure and arrival times of each flight to be within the time intervals which have already been determined by the airline. Time window constraints (9) and (10) can be used to restrict the departure and arrival times of flights within the airlines's own slot times. In this manner, any penalty cost of flights arriving or departing outside of the allocated slot times can be eliminated. Constraint (11) is a Big-M constraint to eliminate the possible nonlinearity. Constraints (12) and (13) define the domain of the variables.

To solve this bi-criteria optimization problem, we use the ϵ-constraint approach (T'kindt and Billaut, 2006). In this approach, we will solve the problem of minimizing $F1$ for a given lower bound on $F2$. We add the following service level bound constraint into the proposed model.

$$\sum_{i \in J} \sum_{j \in P_i} w_{ij} \cdot \gamma_{ij} \geq \gamma \tag{14}$$

In (14), we want the overall service level be greater than or equal to the desired level, γ. The ϵ-constraint method has been widely used in the literature, because the decision maker can interactively specify and modify the service level bounds and analyze the influence of these changes on the total operational cost.

2.1.1. Service level

In this paper, we generate a schedule which is robust to variability at congested airports by increasing passenger service levels. Random variable representing non-cruise times arises in chance constraints (5). Constraint (5) ensures the minimum passenger connection time TP_{ij} between the arrival of flight i and departure of flight j with a probability greater than or equal to γ_{ij}. In constraint (6), we wish to keep the service level (γ_{ij}) for each connection greater than or equal to desired lower bound γ_{ij}^{d} , e.g., an airline may prefer to satisfy the international connections with higher probabilities.

One of our aims is to maximize the overall service level through the entire network. The overall service level is calculated as the weighted average of the service level of each connection as defined in the second objective function of $F2$ in (2). To increase the service level for each passenger connection, we allow changes on the flight departure times within the time window given in Constraint (9). In addition, in response to high variability at the congested airports, we can set a higher cruise speed to ensure the passenger connections with a higher service level. Consequently, we wish to achieve a robust schedule, which is less susceptible to unexpected flight delays due to airport congestions.

2.1.2. Distribution of non-cruise times

Deterministic approaches model the random parameters by their expected values. However, expected values may be too far from the certain realizations in practice, thereby resulting plan may perform poorly. One of the uncertainties in flight appears in non-cruise stage, because actual non-cruise time may take longer than expected due to the airport congestions. We represent the non-cruise time of each flight by a random variable.

Arıkan and Deshpande (2012) show that the log-Laplace distribution provides a good-fit to the block time of a flight. For each flight $i \in J$, we assume random variable A_i representing the non-cruise time has log-Laplace distribution with a scale parameter, e^{α} and the tail parameter, $1/\beta_i$. For each flight $i \in J$, we define β_i as a function of the congestion coefficients of the origin and destination airports of flight i. We express β_i as

$$\beta_i = \beta . \left(e_{O_i}\right)^2 \cdot \left(e_{Dn_i}\right)^2$$

where O_i and Dn_i are the origin and destination airports of flight $i \in J$, respectively. Variability is higher at congested airports. Moreover, the mean of the non-cruise times increases at the congested airports. Duran et al. (2015) provide the mean of the random variable A_i as follows

$$E[A_i] = \frac{e^{\alpha}}{(1-\beta_i) \cdot (1+\beta_i)}. \tag{15}$$

2.1.3. Fuel and CO_2 emission cost functions

In this study, we utilize the idea of aircraft speed control to ensure passenger connections. However, speed decisions affect fuel burn. To estimate the fuel burn, we use the cruise stage fuel flow model developed by the Base of Aircraft Data (BADA) (EUROCONTROL, 2012) which is discussed in detail in Appendix. Fuel burn (kg) as a function of cruise time f_i^t (min) can be calculated as

$$F_i^t\left(f_i^t\right) = c_1^{i,t} \cdot \frac{1}{f_i^t} + c_2^{i,t} \cdot \frac{1}{\left(f_i^t\right)^2} + c_3^{i,t} \cdot \left(f_i^t\right)^3 + c_4^{i,t} \cdot \left(f_i^t\right)^2 \tag{16}$$

where coefficients $c_j^{i,t} > 0$, j=1,... ,4, are expressed in terms of aircraft specific fuel consumption and drag as well as the mass of

aircraft, air density and gravitational acceleration. Note that, $F_i^t(f_i^t)$ is a convex function of $f_i^t > 0$.

Fuel cost for flight i operated by aircraft type t can be calculated as

$$FuelCost_i^t(f_i^t) = c_{fuel} \cdot \left(F_i^t(f_i^t)\right) \tag{17}$$

where c_{fuel} is the unit price for jet fuel ($/kg).

International Civil Aviation Organization (*ICAO*) developed standards for aircraft engine emissions, which forces airlines to put more emphasis on calculation of emissions. EUROCONTROL (2001) states that CO_2 emissions are approximately 3.15 times the weight of fuel consumed. Therefore, cost of CO_2 emission can be expressed as a function of cruise time as

$$EmissionCost_i^t(f_i^t) = c_{CO_2} \cdot k \cdot F_i^t(f_i^t) \tag{18}$$

where c_{CO_2} is the unit cost of CO_2 emission ($/kg) and k is CO_2 emission constant.

For each $p \in P$, $i \in J_p$, $t \in T$, we combine the fuel and emission cost functions and redefine them as

$$C_{fuel\&CO_2}^{i,t}(f_i^t) = \begin{cases} \left(c_{fuel} + c_{CO_2} \cdot k\right) & \\ \quad \cdot (c_1^{i,t} \cdot \frac{1}{f_i^t} + c_2^{i,t} \cdot \frac{1}{(f_i^t)^2} + c_3^{i,t} \cdot (f_i^t)^3 & \\ \quad + c_4^{i,t} \cdot (f_i^t)^2) & \text{if } z_p^t = 1 \\ 0 & \text{if } z_p^t = 0 \end{cases}$$

so that if an aircraft of type t is not assigned to path p, then $C_{fuel\&CO_2}^{i,t}(f_i^t) = 0$ $i \in J_p$.

Fuel consumption function $F_i^t(f_i^t)$ is minimized at Maximum Range Cruise (MRC) speed. Although the most fuel efficient case is to fly at MRC speed, airlines sometimes prefer to fly at a higher speed to ensure the aircraft and passengers' connections.

2.1.4. Objectives

In this paper, we deal with a bi-criteria optimization problem of simultaneously minimizing airline's operational costs, denoted as $F1$ in (1), and maximizing service level for passenger connections, denoted as $F2$ in (2), in the proposed nonlinear mathematical model. To satisfy the passenger connections with a higher service level, we may employ both idle time insertion and cruise time compression, or only use one of them based on their impact on operational cost. In order to decrease fuel and emission costs, we may assign a fuel efficient but smaller aircraft to flights whose cruise times need to be compressed. Although we spill some of the passengers, we may compensate the cost of spilled passengers by conservation of fuel. Therefore, we simultaneously consider these interrelated cost terms such as fuel and emission costs, idle time insertion costs and cost of spilled passengers to achieve a minimum cost schedule.

For flight i, aircraft type t, we express idle time cost function as

$$C_{idle}^{i,t}(S_i^t) = S_i^t \cdot I^t \tag{19}$$

Similarly, we represent cost of spilled passengers with a linear function of the number of passengers who cannot be accommodated and turned away by the airlines due to the insufficient seat capacity of aircraft. For flight i, aircraft type t, spilled passenger cost can be expressed as

$$C_{spilled}^{i,t} = Csp_i \cdot max\left(D_i - CAP^t, 0\right) \cdot z_p^t \tag{20}$$

2.2. Numerical example

In this section, a numerical example is provided to illustrate how fuel consumption and CO_2 emission of aircraft affect the assignment decisions and how the cruise time controllability and idle time insertion can be utilized to generate a robust schedule.

In this small example, we consider two given paths operated by two different aircraft. Table 1 shows the tail numbers and flight numbers along with the origin and destination airports, planned departure times, planned block and arrival times, actual arrival times, turnaround times, and demand of flights. Two flights with the same flight number, 336, represents a through flight that includes one or more intermediate airports between the origin and destination airports. The first path including flights 2303, 2336, 1053 and 336 is operated by Boeing 737 500 and the second path is flown by MD 83. While aircraft is flying at MRC speed, fuel burn rates of B737 500 and MD 83 are estimated as 29 kg/min and 40 kg/min, respectively. The fuel burn rate is calculated using the fuel flow model of BADA as in Eq. (46) in Appendix.

In daily operations, some flights may not be operated as planned. One reason is that a flight may take longer than the expected duration. In the published schedule, let's assume that 25 min of the flight duration is planned non-cruise time and remaining is planned cruise time. However, non-cruise time has an expected value of 28 min for flight 2303, when we represent non-cruise times with a log-Laplace random variable. We calculate the expected value as in Eq. (15) with α taken as log(20) and β taken as 0.05. Therefore, actual flight duration is 2 h 33 min, so that the actual arrival time is 9:08 which is 3 min later than planned arrival time. In the published schedule given in Table 1, some time is left between the arrival and departure times of consecutive flights of each aircraft. If this time is not enough to prepare an aircraft for the next flight, there will be some delays on departure of next flight. Such delays may result in passenger misconnections. On the other hand, if this time is longer, there exists idle times between the consecutive flights. For example, time between planned arrival of flight 1131 and planned departure of flight 1339 is 65 min. An aircraft requires 36 min to be prepared for next flight 1339. Therefore, 29 min between these consecutive flights are enough to capture 3 min of delay on arrival of flight 1131. In other words, 26 min of idle time remains between flights 1131 and 1339.

The time-space network diagram of the published schedule in Table 1 is given in Fig. 1. In Fig. 1 continuous arcs represent planned flights, where the dashed arcs represent actual flight times. The blue and red arcs in Fig. 1 are for aircraft N531AA and N454AA, respectively. Turnaround times of the aircraft are represented by the continuous ground lines and idle times are represented by the dashed ground lines.

Fig. 1, departure of the first leg of flight 336 is delayed, since there is not enough time between actual arrival of flight 1053 and planned departure of flight 336 to prepare an aircraft for flight 336. On the other hand, there exist 18 min idle times before departure of flight 1053. Therefore, published schedule needs a better utilization of idle times by re-timing departure times as already discussed in Ahmadbeygi et al. (2010). Re-timing approach can be used to increase passenger connection possibilities. We also use the idea of speeding up some aircraft especially at congested airports to ensure passenger connections at a desired service level. However, we should consider adverse effect of speeding up aircraft on fuel and carbon emission costs. If we assign a fuel efficient aircraft to a flight, reduction in fuel cost may compensate the cost of idle time insertion. On the other hand, this assignment may incur an additional cost of spilled passengers. The objective function of the integrated model (IM) considers these four conflicting cost components of the schedule. The new schedule achieved by IM is provided in Fig. 2.

In Fig. 2, we see that aircraft assignments among two paths are switched compared to the published schedule. Red and blue arcs in Fig. 2 are for aircraft N531AA and N454AA, respectively. integrated model assigns fuel efficient aircraft B737 500 to the second path. Our approach compresses cruise time durations of flights 2441, 1986, 1872 and 1131 by 10, 10, 12 and 12 min, respectively.

Table 1
Published schedule.

Tail #	Flight #	From	To	Plan. dep.	Plan. dur.	Plan. arr.	Act. arr.	TA	Demand
N531AA	2303	ORD	DFW	6:35	2:30	9:05	9:08	0:48	121
	2336	DFW	ORD	10:00	2:35	12:35	12:38	0:49	117
	1053	ORD	ATL	13:45	2:05	15:50	15:50	0:47	110
	336	ATL	ORD	16:30	2:10	18:40	18:47	0:25	120
	336	ORD	LGA	19:20	2:15	21:35	21:37		112
N454AA	2441	ORD	ATL	6:45	2:10	8:55	8:55	0:33	118
	1986	ATL	ORD	09:40	2:15	11:55	11:55	0:36	121
	1872	ORD	DFW	12:35	2:30	15:05	15:08	0:34	129
	1131	DFW	ORD	15:50	2:35	18:25	18:28	0:36	122
	1339	ORD	SAN	19:30	4:30	00:00	23:56		146

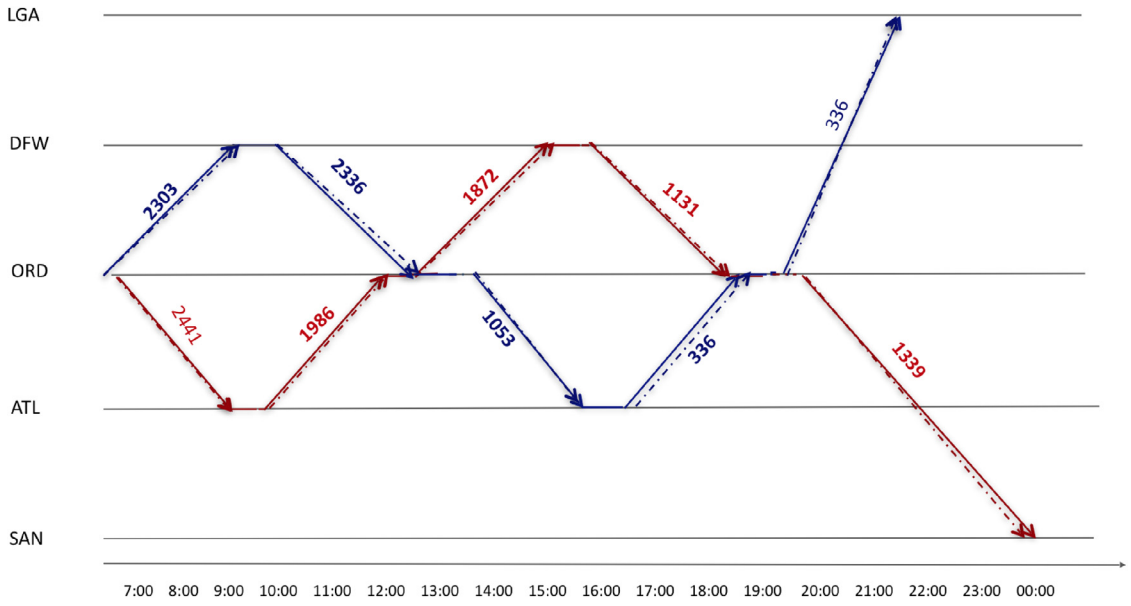

Fig. 1. Time Space Network for the Published Schedule. (For interpretation of the references to colour in the text, the reader is referred to the web version of this article.)

The reason of speeding up the aircraft is that, passengers of flight 1131 have connections to the second leg of flight 336. The crucial point is that total compression amount of 44 min is not imposed upon only on flight 1131. Due to the nonlinearity of fuel cost function, it is more beneficial to allocate the required compression to multiple flights. In Fig. 2, continuous arcs represent flights operated under the MRC speed, where dashed lines refer to flights with compressed cruise times.

Speeding up aircraft may not be enough to satisfy passenger connections at a desired service level. Therefore, 16 min of idle time is also inserted before flight 336 to satisfy passenger connections between flights 1131 and 336. The reason for utilizing both speed control and idle time insertion is that speeding up the aircraft might be cheaper than idle time insertion up to a point, and then idle time insertion might be cheaper due to the nonlinearity of fuel cost function.

We compare the performance of new schedule with the published schedule in terms of operational costs. Fuel and CO_2 emission costs are calculated as explained in Eqs. (17) and (18), respectively. Idle time costs are calculated by multiplying total idle time with the unit idle cost of aircraft, which is given in Table 5. The cost of spilled passengers are also calculated as multiplying total number of spilled passengers with the unit cost which is calculated as in Eq. (44).

Table 2 shows the improvements in fuel and emission cost, idle time insertion cost and total cost compared to the published schedule. We assume that aircraft speed is constant in the published schedule. In our approach, we use the option of flying faster

Table 2
Cost comparison.

	Fuel & emission cost ($)	Idle cost ($)	Spilled cost ($)	Total cost ($)
Published schedule	56,196	11,173	0	67,369
Integrated model (IM)	54,841	4,766	708	60,315

to satisfy the passenger connections. However, speeding up the aircraft incurs additional fuel and emission costs. By considering fuel burn and carbon emission costs, integrated model switches the assignment of aircraft types among two paths compared to published schedule. By this fleet assignment, we obtain 2.5% cost saving in fuel consumption and CO_2 emissions compared to the published schedule. Total fuel and CO_2 emission costs for the published schedule and new schedule are $56,196 and $54,841, respectively. On the other hand, this assignment spills 31 passengers of total 1,216 passengers, which costs $708. In addition to speeding up aircraft, to satisfy the passenger connections at 90% service level, 17 min and 16 min of idle times are also inserted before flight 1053 and second leg of flight 336. Therefore, there exists total 33 min of idle time in the new schedule, whereas there exists 80 min of idle time in the published schedule. Our proposed model eliminates the unnecessary idle times and reallocates the required amount of slack among the flights with controllable cruise time decisions so that passenger connections are satisfied at desired service level. It follows that new schedule results in 57% improvement in idle time cost, where the costs of the idle time in the published sched-

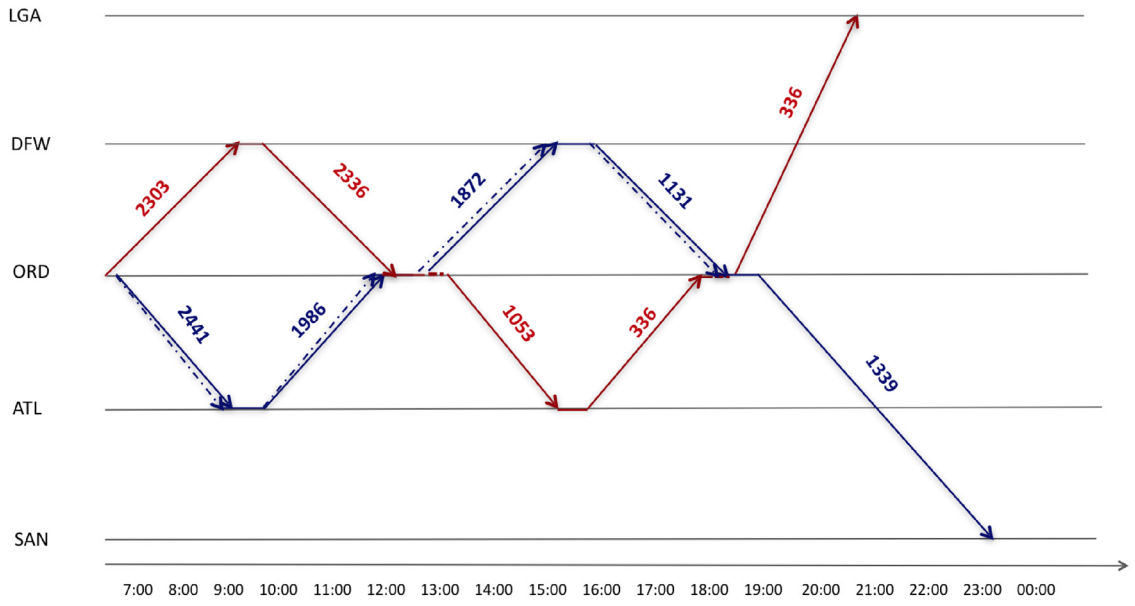

Fig. 2. Time Space Network - by IM.

ule and new schedule are $11,173 and $4,766, respectively. In total, operational cost saving is around 10% compared to the published schedule.

3. Conic reformulation of integrated model

Our model involves nonlinear fuel and carbon emission cost terms in the objective function and chance constraints. Nonlinear mixed integer optimization often requires significant computation time to achieve optimal or suboptimal solutions. To reduce the computation time, in this section, we utilize conic quadratic programming.

3.1. Conic representation of chance constraints

In this study, we ensure passenger connections through chance constraints with a desired service level. In the literature, most of the studies handle the chance constraints with approximation methods. In this section, we show how to reformulate the chance constraints via second order conic inequalities.

The random variable representing non-cruise time of a flight arises in chance constraints. For each flight $i \in J$, we assume that random variable A_i representing non-cruise time has Log-Laplace distribution. The density and quantile function of the Log-Laplace distribution can be found in Appendix.

Constraint (5) can be expressed using the quantile function of the probability distribution of random variable A_i with parameters e^{α} and $1/\beta_i$ as follows:

$$\frac{e^{\alpha}}{2^{\beta_i}\cdot(1-\gamma_{ij})^{\beta_i}} \le x_j - x_i - TP_{ij} - \sum_{t\in T} f_i^t, \qquad \text{if} \quad \frac{1}{2} \le \gamma_{ij} \le 1 \tag{21}$$

In this study, we wish to keep each service level greater than or equal to 50%, this is the reason why we consider the quantile function for $0.5 \le \gamma_{ij}$ in constraint (21). Duran et al. (2015) achieve the convexity of the expression on the left hand side of inequality (21). Then, Proposition 1 gives the conic representation of the constraint (21).

Proposition 1. *For $i \in J$, $j \in P_i$, if $0 < \beta_i < 1$ and $\frac{1}{2} \le \gamma_{ij} \le 1$, then constraint (21):*

$$\frac{e^{\alpha}}{2^{\beta_i}\cdot(1-\gamma_{ij})^{\beta_i}} \le x_j - x_i - TP_{ij} - \sum_{t\in T} f_i^t,$$

can be represented via second order conic inequalities.

Proof. The proof is similar to the proof of Proposition 2 in Duran et al. (2015). In their study, fleet types are taken as fixed parameters and cruise times are represented by f_i for each flight $i \in J$. In this study, cruise times represented by f_i^t vary among fleet types. Therefore, in their proof, we can replace f_i with $\sum_{t\in T} f_i^t$, since $f_i^t = 0$ if the $z_p^t = 0$. Then, we obtain the following hypograph.

Let the constant $\lambda = \frac{e^{\alpha}}{2^{\beta_i}}$ and $\beta_i = \frac{a_i}{b_i}$ for integers a_i and b_i. Choose l such that $l = \lceil \log_2(a_i + b_i) \rceil$. Then, chance constraints in the original formulation can be replaced by the following constraints for $i \in J$, $j \in P_i$:

$$\begin{aligned} (x_j - x_i - TP_{ij} - \sum_{t\in T} f_i^t) &= \sigma_{ij} \\ \overline{\gamma}_{ij} &= 1 - \gamma_{ij} \\ \sigma_{ij}^{\,b_i} \cdot \overline{\gamma}_{ij}^{\,a_i} &\ge (\sqrt[2^l]{\lambda^{b_i}})^{2^l} \end{aligned} \tag{22}$$

Due to Ben-Tal and Nemirovski (2001), the hypograph of the geometric mean of 2^l variables can be represented via second order conic inequalities. In (22), it can be seen that b_i of the variables equal to σ_{ij}, a_i of the variables equal to $\overline{\gamma}_{ij}$ and the remaining $2^l - a_i - b_i$ variables can be set to 1. Hence, it is clearly observed that constraint (22) represents the hypograph of the geometric mean of 2^l variables. According to Ben-Tal and Nemirovski (2001), the hypograph can be equivalently represented by hyperbolic inequalities of the form,

$$u^2 \le v_1 v_2, \qquad u, v_1, v_2 \ge 0$$

which can be represented by the second order conic inequality below

$$\|(2u, v_1 - v_2)\| \le v_1 + v_2$$

that concludes the proof. □

3.2. Conic representation of fuel and CO_2 cost functions

In this section, we show conic quadratic reformulation of fuel burn and carbon emission cost functions. To simplify the presentation, we drop the indices of the variables and parameters as follows:

$$C_{fuel\&CO_2}(f) = \begin{cases} (c_{fuel} + c_{CO_2} \cdot k)(c_1 \cdot \frac{1}{f} \\ \quad + c_2 \cdot \frac{1}{f^2} + c_3 \cdot f^3 + c_4 \cdot f^2) & \text{if } z = 1 \\ 0 & \text{if } z = 0 \end{cases}$$

$C_{fuel\&CO_2}(f)$ is discontinuous and therefore its epigraph $E_F = \left\{(f,t) \in R^2 : C_{fuel\&CO_2}(f) \le t\right\}$ is nonconvex. In the next proposition, we describe how the convexity of E_F is obtained. A more detailed information can be found in Aktürk et al. (2014) and Günlük and Linderoth (2010).

Proposition 2. *The convex hull of E_F can be expressed as*

$$t \ge (c_{fuel} + k \cdot c_{CO_2})(c_1 \cdot q + c_2 \cdot \delta + c_3 \cdot \varphi + c_4 \cdot \vartheta) \tag{23}$$

$$z^2 \le q \cdot f \tag{24}$$

$$z^4 \le f^2 \cdot \delta \cdot z \tag{25}$$

$$f^4 \le z^2 \cdot \varphi \cdot f \tag{26}$$

$$f^2 \le \vartheta \cdot z \tag{27}$$

in the constraint set. Moreover, each inequalities (24)–(27) can be represented by conic quadratic inequalities.

Proof. Perspective of a convex function $k(f)$ is $z \cdot k(f/z)$ (Hiriart-Urruty and Lemarećhal, 2001). Since each of the nonlinear terms $\frac{1}{f}$, $\frac{1}{f^2}$, f^3 and f^2 is a convex function for $f \ge 0$, then epigragh of the perspective of each term can be stated as, $\frac{z^2}{f} \le q$, $\frac{z^4}{f^2} \le \delta$, $\frac{f^3}{z^2} \le \varphi$, $\frac{f^2}{z} \le \vartheta$ respectively. Since $z, f \ge 0$, they can be written as stated in the proposition.

Finally, observe that (24) and (27) are hyperbolic inequalities, (25) can be restated as two hyperbolic inequalities

$$z^2 \le w \cdot f \quad \text{and} \quad w^2 \le \delta \cdot z$$

and (26) can be restated as

$$f^2 \le w \cdot z \quad \text{and} \quad w^2 \le \varphi \cdot f$$

which can be written as a conic quadratic inequality as described in Section 3.1. □

3.3. Conic reformulation of integrated model

The model can be reformulated using the hyperbolic inequalities which can be written as conic quadratic inequalities as follows:

$$\min \quad \sum_{i\in J}\sum_{t\in T}\left(c_{fuel} + c_{CO_2} \cdot k\right)\left(c_1 \cdot q_i^t + c_2 \cdot \delta_i^t + c_3 \cdot \varphi_i^t + c_4 \cdot \vartheta_i^t\right) + \sum_{p\in P}\sum_{i\in J_p}\sum_{t\in T} Csp_i \cdot max\left(D_i - CAP^t, 0\right) \cdot z_p^t + \sum_{i\in J}\sum_{t\in T} S_i^t \cdot I_i^t$$

$$\text{s.to} \tag{28}$$

$$(3) - (4)$$

$$\left(z_p^t\right)^2 \le q_i^t \cdot f_i^t \qquad i \in J_p,\ p \in P,\ t \in T \tag{29}$$

$$\left(z_p^t\right)^4 \le \left(f_i^t\right)^2 \cdot \delta_i^t \cdot z \qquad i \in J_p,\ p \in P,\ t \in T \tag{30}$$

$$\left(f_i^t\right)^4 \le \left(z_p^t\right)^2 \cdot \varphi_i^t \cdot f_i^t \qquad i \in J_p,\ p \in P,\ t \in T \tag{31}$$

$$\left(f_i^t\right)^2 \le \vartheta_i^t \cdot z_p^t \qquad i \in J_p,\ p \in P,\ t \in T \tag{32}$$

$$\sigma_{ij}{}^{b_i} \cdot \overline{\gamma}_{ij}{}^{a_i} \ge \left(\sqrt[2^l]{\lambda^{b_i}}\right)^{2^l} \qquad i \in J,\ j \in P_i \tag{33}$$

$$x_j - x_i - TP_{ij} - \sum_{t\in T} f_i^t = \sigma_{ij} \qquad i \in J,\ j \in P_i \tag{34}$$

$$\overline{\gamma}_{ij} = 1 - \gamma_{ij} \qquad i \in J,\ j \in P_i \tag{35}$$

$$\sum_{i\in J}\sum_{j\in P_i} w_{ij} \cdot \gamma_{ij} \ge \gamma \tag{36}$$

$$(6) - (13)$$

Objective function (28) is slightly different than the original objective function of the proposed model. The original objective, $F1$ is represented by the new objective and conic constraints (29)–(32). ϵ-constraint approach is implemented by Constraint (36) which imposes a lower bound on $F2$. The probabilistic constraints (5), are represented by the conic constraints (33)–(35). The remaining constraints are same as the original constraints of the proposed model.

4. Algorithm for aircraft-path assignment and robust airline scheduling

Integrated aircraft-path assignment and schedule design is a very complex problem with nonlinear cost terms, chance constraints and binary aircraft assignment decisions. To mitigate the computational difficulties, we utilize mixed integer second order cone programming. However, in real size problems, the vast number of re-timing and re-fleeting decisions may still require problems to be broken into smaller subproblems to efficiently manage tractability. Traditional approaches adopt a sequential planning process. First, decisions of a flight schedule are made, and then assignment of airline's fleet to scheduled flights is determined. Even though sequential planning approach greatly simplifies the solution process, it could create incompatibilities between various stages. For example, a flight schedule in the first stage may not be feasible for aircraft and passenger connections in the subsequent stages. Therefore, we present an approach that incorporates decisions of a downstream stage into an upstream model and vice versa. Our two-stage approach decomposes the problem into planning stages such as aircraft-path assignment defined in Section 4.1 and robust airline scheduling defined in Section 4.2. In each iteration, two-stage algorithm solves each subproblem by giving the output of one subproblem as an input for other subproblem. In the first subproblem, we assign aircraft types to paths for a given flight schedule with departure times, cruise times and idle times. In the second subproblem, we impose assignment decisions into the robust airline scheduling model, and then construct a flight schedule with departure times, cruise times and idle times.

We first give the steps of two-stage Algorithm 1. Algorithm 1 starts with an initial schedule Sch_1, and given cruise times $\vec{f}_1$ and idle times $\vec{S}_1$ of the schedule Sch_1. With given cruise and idle times, the algorithm applies the `Construction` algorithm to generate a new schedule by iteratively solving the

Algorithm 1 Two-stage algorithm.

Require: An initial schedule Sch_1, cruise times $\vec{f}_1$ and idle times $\vec{S}_1$ for each flight.
Initialize: `found_improving_move` ← **false**.
$Sch^* \leftarrow Sch_1$. Iteration index `k` ← 1. Tabu list is empty, TL = {}.
Apply `Construction` Algorithm.
Report the generated solution.
repeat
  Apply `Improvement` Algorithm.
  Report the generated solution.
until `found_improving_move` is **false**.

aircraft-path assignment problem defined in Section 4.1 and robust airline scheduling problem defined in Section 4.2, and then records the solution. The next step is to apply `Improvement` algorithm by changing the fleet assignment sequences and solving the robust airline scheduling problem again. The algorithm terminates when no further reduction in overall operational cost can be attained. In the following, we will describe two subproblems, which motivates the construction and improvement algorithms, and then we will describe the steps of Algorithm 1 in detail.

4.1. Subproblem 1: Aircraft-Path assignment problem

We first define aircraft-path assignment problem. The solution to the subproblem is an input for `Construction` algorithm. Given cruise times $\vec{f}_k$ and idle times $\vec{S}_k$ of the schedule S_k, aircraft-path assignment problem finds an optimal fleet assignment sequence $\vec{z}_k$ to flight paths without assigning an aircraft more than once such that all paths are covered. The objective is to minimize the overall operational cost of the schedule. The problem is formulated as follows:

$$AAM(\vec{f},\vec{S}): \min \quad \sum_{p\in P}\sum_{t\in T} TC_p^t(\vec{f},\vec{S})\cdot z_p^t \tag{37}$$

$$\text{s.to} \quad \sum_{t\in T} z_p^t = 1 \quad p\in P \tag{38}$$

$$\sum_{p\in P} z_p^t \le N^t \quad t\in T \tag{39}$$

$$z_p^t \in \{0,1\} \quad p\in P, t\in T \tag{40}$$

where the total cost $TC_p^t(\vec{f},\vec{S})$ involving the costs of fuel consumption and CO_2 emission, cost of spilled passengers and cost of idle time for each path $p \in P$ and for each aircraft type $t \in T$ is calculated as follows:

$$\begin{aligned} TC_p^t(\vec{f},\vec{S}) &= \sum_{i\in J_p}\left(c_{fuel}+c_{CO_2}\cdot k\right) \\ &\cdot\left(c_1^{i,t}\cdot\frac{1}{\vec{f}_i^t}+c_2^{i,t}\cdot\frac{1}{\left(\vec{f}_i^t\right)^2}+c_3^{i,t}\cdot\left(\vec{f}_i^t\right)^3+c_4^{i,t}\cdot\left(\vec{f}_i^t\right)^2\right) \\ &+\sum_{i\in J_p} Csp_i\cdot max\left(D_i-CAP^t,0\right)+\sum_{i\in J_p}\vec{S}_i^t\cdot I^t \end{aligned} \tag{41}$$

4.2. Subproblem 2: Robust airline scheduling problem

We define another subproblem robust airline scheduling problem. The solution of this subproblem is an input for both `Construction` and `Improvement` algorithms. Given a fleet assignment sequence $\vec{z}_k$ to paths, robust airline scheduling problem finds optimal cruise times $\vec{f}_k$ and idle times $\vec{S}_k$ while ensuring the desired passenger connection service level. We achieve robustness by ensuring passenger connections at a desired service level via introducing time windows on departures and controlling cruise speed, by leaving the fleeting decisions unchanged. The objective is to minimize fuel consumption and CO_2 emission costs and idle times cost. The problem is formulated as follows:

$$\begin{aligned} RASM\left(\vec{z}\right): \min \quad & \sum_{p\in P}\sum_{i\in J_p}\sum_{t\in T} C_{fuel\&CO_2}^{i,t}\left(f_i^t\right) \\ &+\sum_{p\in P}\sum_{i\in J_p}\sum_{t\in T} Csp_i\cdot\max\left(D_i-CAP^t,0\right)\cdot\vec{z}_p^{\,t} \\ &+\sum_{i\in J}\sum_{t\in T} S_i^t\cdot I_i^t \end{aligned} \tag{42}$$

$$\text{s.to} \quad \sum_{i\in J}\sum_{j\in P_i} w_{ij}\cdot\gamma_{ij}\ge\gamma \tag{43}$$

$$(5)-(12)$$

$RASM(\vec{z})$ is a nonlinear model of probabilistic constraints and nonlinear cost components. Exact and fast solutions are obtained by the use of second order conic programming reformulations as discussed in the previous section.

4.3. Construction algorithm

Algorithm 2 gives the `Construction` algorithm. The algorithm starts with an initial schedule and given cruise times and idle times. Afterwards, it solves Aircraft-Path Assignment subproblem to find an optimal fleet assignment sequence to minimize the overall operational cost. The optimal fleet assignment sequence is imposed upon the Robust Airline Scheduling subproblem to find the optimal cruise times and idle times corresponding the optimal fleet assignment sequence. This procedure iteratively continues to obtain schedules with improved operational cost. The algorithm terminates when it is stuck in the same fleet assignment sequence.

In the `Construction` algorithm, there may exist some incompatibilities between two subproblems, which arise as an inevitable consequence of sequential planning approach. For instance, schedule generated by the RASM may not be feasible for aircraft connections of the subsequent fleet assignment. The main reason of this infeasibility is that the RASM ensures aircraft connections by considering turnaround time requirement for only the fleet assignment solution of the previous AAM. Any fleet assignment different than the previous one may require longer turnaround times, thus

Algorithm 2 Construction algorithm.

Require: An initial schedule Sch_1, cruise times $\vec{f}_1$ and idle times $\vec{S}_1$ for each flight.
Initialize: `changed_assignment` ← **true**. $Sch^* \leftarrow Sch_1$. Iteration index `k` ← 1;
while `changed_assignment` **do**
  Solve $AAM(\vec{f}_{k-1},\vec{S}_{k-1})$;
  New fleet assignment sequence is $\vec{z}_k$;
  Solve $RASM(\vec{z}_k)$;
  New schedule is Sch_k
  Report the generated solution $\vec{f}_k$ and $\vec{S}_k$;
  if $COST(Sch_k,\vec{z}_k) < COST(Sch^*,\vec{z}^*)$ **then**
    $Sch^* \leftarrow Sch_k$;
    $\vec{z}^* \leftarrow \vec{z}_k$
  else
    if $\vec{z}_k == \vec{z}^*$ **then**
      `changed_assignment` ← **false**;
  `k` ← `k`+1;

resulting in aircraft misconnections. To decrease these incompatibilities, we resolve the RASM to generate a new feasible solution by taking the fleet assignment, for which the previous schedule is infeasible, as an input. When the AAM model produces the same fleet assignment as the best one found so far, `Construction` algorithm terminates. This could be a local solution for the problem. To explore different fleet assignment sequences, in the next section, we describe a neighbourhood search procedure which is used by an `Improvement` algorithm.

4.4. All pairwise interchange

To explore a larger solution space, one of the most common approaches in the scheduling literature is the pairwise interchange method. This method compares the cost of two fleet assignment sequences which differ only by interchanging a pair of fleet with two different types. We will explain how to generate many fleet assignment sequences from one fleet assignment sequence with a small example. Let the best fleet type assignment sequence for four paths be $\vec{z}^*$:= (1, 2, 2, 3) where numbers 1, 2 and 3 correspond to the fleet types. All Pairwise Interchange Method produces the following five fleet type assignment sequences; $\vec{z}_1$ = (2, 1, 2, 3), $\vec{z}_2$ = (2, 2, 1, 3), $\vec{z}_3$ = (3, 2, 2, 1), $\vec{z}_4$ = (1, 3, 2, 2), $\vec{z}_5$ = (1, 2, 3, 2). For example, the first assignment sequence, $\vec{z}_1$ is constructed by interchanging fleet 1 and 2 between 1st and 2nd paths.

We generate many fleet assignment sequences at each iteration of the `Improvement` algorithm. The question is which fleet type assignment sequence will be selected at each iteration. The rule is to select the one with the smallest overall operational cost. The costs of the schedule S^* with many different fleet type assignment sequences are calculated using formula (41).

4.5. Improvement algorithm

Algorithm 3 gives the `Improvement` algorithm. The algorithm starts with the schedule which is generated by `Construction` algorithm and iteratively applies `All Pairwise Interchange` to generate a neighbourhood involving different fleet assignment sequences. Algorithm 3 selects the most promising fleet assignment sequence by solving *RAS* problem and comparing the cost of corresponding schedules. Therefore, a schedule with improved cost is obtained at each iteration of the algorithm. A reverse move of the improving move of the fleet assignment sequence $\vec{z}^* \leftarrow \vec{z}_{i^*}$ is added to the top of the tabu list to prevent cycling. If tabu list is longer than L, the last entry is removed from the tabu list. Algorithm terminates when no improvement is possible for the current schedule.

In this section, we have described a heuristic algorithm which decomposes the problem into two planning stages, such as aircraft assignment and robust airline scheduling, and then solves them sequentially. Unfortunately, a sequential approach eliminates the interdependencies, thus resulting in a suboptimal solution or even infeasible solution. To reduce incompatibilities between subproblems, decisions of the schedule design problem are imposed upon the aircraft assignment model, whereas decisions of aircraft-path assignment problem are imposed upon the robust airline scheduling model in each iteration. In the next section, using data of a major U.S. airline, we show that our two-stage approach is both tractable and capable of producing very promising results to the aircraft-path assignment and robust airline scheduling problem.

5. Computational results

In our computational study, we test the performance of mixed integer second order conic programming formulation introduced in Section 3 and two-stage algorithm introduced in Section 4. We

Algorithm 3 Improvement algorithm.

Require: A given schedule Sch^*, cruise times $\vec{f}^*$, idle times $\vec{S}^*$ and $\vec{z}^*$.
Initialize: `improving_move` ← **true**;
while `improving_move` **do**
  Generate a neighborhood N around $\vec{z}^*$ using all pairwise interchange;
  Calculate $Cost(Sch^*, \vec{z}^*_i)$ forall $i \in N$;
  Select m fleet assignment $\vec{z}^*_1, \vec{z}^*_2, \ldots, \vec{z}^*_m$ which give the minimum $Cost(Sch^*, \vec{z}^*_i)$ forall $i \in N$;
  if any of the moves $\vec{z}^* \rightarrow \vec{z}^*_1$, $\vec{z}^* \rightarrow \vec{z}^*_2 \ldots$, and $\vec{z}^* \rightarrow \vec{z}^*_m$ is prohibited by a move on the tabu list **then**
    Eliminate that one from the neighborhood N;
    Select the $(m+1)^{st}$ fleet type assignment $\vec{z}^*_{m+1}$ with minimum cost;
  Solve $RASM(\vec{z}^*_i)$ for $i = 1, 2, \ldots, m$;
  New schedule is Sch_i for $i = 1, 2, \ldots, m$;
  Select i^* with minimum $Cost(Sch^*, \vec{z}^*_i)$ for $i = 1, 2, \ldots, m$.
  if $Cost(Sch^*, \vec{z}^*_{i^*}) < Cost(Sch^*, \vec{z}^*)$ **then**
    $Sch^* \leftarrow Sch_{i^*}$;
    $\vec{z}^* \leftarrow \vec{z}_{i^*}$;
    if $Lengthof TL < L$ **then**
      $TL = TL \bigcup \{\vec{z}_{i^*} \rightarrow \vec{z}^*\}$;
    else
      Remove the last entry;
      $TL = TL \bigcup \{\vec{z}_{i^*} \rightarrow \vec{z}^*\}$;
    `improving_move` ← **true**
  else
    `improving_move` ← **false**

Table 3
Factor values.

	Levels	
Factor description	Low	High
C_{fuel} ($/kg)	0.6	1.2
Base Spill Cost ($/passenger)	15	60
β	0.01	0.05

test these two approaches on three different schedules generated from the work of Aktürk et al. (2014). The flight information is extracted from database "Airline On-Time Performance Data," provided by the Bureau of Transportation Statistics of the US Department of Transportation, BTS (2010a). We perform experiments in Sections 5.1 and 5.2 on a 64-bit Windows 7 computer with 8 GB memory and Intel Xeon E5640 2.67 GHz CPU. We implement the conic quadratic mixed integer reformulation and the two-stage algorithm in JAVA programming language with a connection to commercial solver IBM ILOG CPLEX Optimization Studio 12.5. Then, we perform the experiments in Section 5.3 on a OS X Yosemite computer with 8 GB memory and 2,6 GHz Intel Core i5 processor and use commercial solver IBM ILOG CPLEX Optimization Studio 12.6.

In order to analyze the effects of problem parameters, we conduct a 2^k full-factorial experimental design. The experimental factors are chosen and their levels are given in Table 3.

C_{fuel} is the price of jet fuel per kg. History of fuel prices obtained from IATA fuel price monitor IATA (2014) indicates that price of one kilogram fuel is fluctuating between $0.5 and $1.26 in 2015. In this study, fuel prices are taken as $0.6/kg and $1.2/kg for lower and higher settings, respectively.

Base Spill Cost represents the opportunity cost for each of spilled passengers due to the insufficient seat capacity of the aircraft. Number of spilled passengers is directly affected by the fleet assignment decisions. In order to assess the overall impact of the

number of spilled passengers on the airline's operating cost as depicted as $F1$ in (1) in the proposed formulation, we have selected the base spill cost as an experimental factor in our computational settings and its corresponding low and high levels as shown in Table 3. Afterwards, the cost of spilled passengers is adjusted for each flight using airport congestion coefficients, e.g. favoring the populated markets, as shown in Eq. (44).

$$Csp_i = BaseSpillCost \cdot \left(e_{O_i}\right) \cdot \left(e_{Dn_i}\right) \tag{44}$$

The third experimental factor, β, is used for the tail parameter of Log-Laplace distribution. Duran et al. (2015) state that the highest possible value of β is 0.07 to ensure that tail parameter $\beta_i > 1$ for each flight $i \in J$ needed to have finite expected values. Therefore, we analyze the performance of the schedule by setting β values as 0.01 and 0.05 under the low and high settings, respectively. With a scale parameter, e^{α}, the tail parameter is used to expect the mean and variance of the random variable. In this study, the scale parameter, e^{α} is taken as 20 to have a non-cruise time deviating from 20 min.

To be used for computational purposes, we construct a sample of flight schedules in Table 4 from the work of Aktürk et al. (2014). We queried the planned departure and arrival times of a commercial airline flights for a single day. Then, we filtered the schedule such that an aircraft first departs from Chicago O'Hare International Airport (ORD) and revisits ORD at least once on the same day. This allows us to work on a schedule of flights, which has passenger connections at such congested airports. The schedule has 114 flights operated by 32 different aircraft. In this study, to observe the effect of seat capacity and fuel efficiency of the aircraft on the fleet assignment, we consider randomly selected six different aircraft types. A group of flights under the same tail number represents an aircraft path operated by the same aircraft. For the computational study, we adopt the fuel burn model of BADA (EUROCONTROL, 2012) mentioned in Section 2.1.3. The fuel consumption coefficients of an aircraft are taken from operational performance files provided by BADA (EUROCONTROL, 2012). For six different aircraft types, we list the fuel burn related parameters, corresponding MRC speed and seat capacity in Table 5. Base turn times of aircraft are adopted from airplane characteristics of Boeing company Boeing. We have used the initial investment cost of each aircraft type to estimate the idle time cost of each aircraft type in dollars per minute as summarized in Table 5.

We generate passenger demand uniformly between 110 and 134, 110 and 122, 110 and 148, 150 and 172, 160 and 180, 160 and 218, if originally assigned aircraft types in the published schedule are B727 228, B737 500, MD 83, A320 111, A320 212 and B767 300, respectively. We can assume that the original aircraft assignment satisfies all passenger demand. Under this experimental setting, we can clearly analyze the performance of aircraft assignment considering the fuel efficiency of the aircraft as well as the passenger demand compared to an assignment decision solely focusing on the passenger demand satisfaction.

In the computational study, we compare the schedule generated by our model to the published schedule in Table 4. We make some assumptions on the published schedule, such that 20 min of the flight times in the published schedule in Table 4 are taken as planned non-cruise times and remaining is planned cruise time. For example, planned flight time for flight 2303 is 155 min. 135 min of the flight time are assumed to be the planned cruise times and 20 min are planned non-cruise times in the published schedule. In our model, we represent the non-cruise times with a random variable which has a log-Laplace distribution. To be consistent with the published schedule, we take the scale parameter, e^{α} of the random variable as 20 to have a non-cruise time deviating from 20 min. We calculate the cruise length by multiplying MRC speed of originally assigned fleet type with planned cruise time under the assumption that speed is constant during the cruise stage. We also calculate the upper bound $f_i^{u,t}$ for cruise times by dividing the cruise length of flight, i with MRC speed of the aircraft, t. In our model, we allow compression on cruise times by 15% of $f_i^{u,t}$.

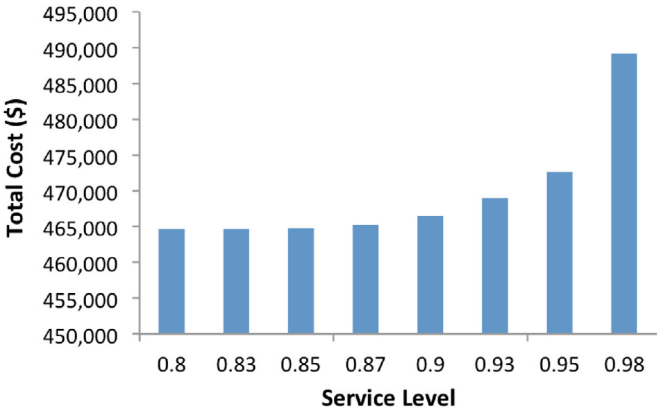

Fig. 3. What if Analysis on the Service Level.

We add a generated passenger connection network to the published schedule. We construct a set P_i to represent flights which have a passenger connection with flight i. We include flight j in set P_i, if the original departure time of flight j in the published schedule is within 45 min or 180 min of the original arrival time of flight i and destination airport of flight i is same as the origin airport of flight j. Passenger connection times, TP_{ij} in constraint 5 are taken uniformly between 25 and 40 min. The weights of the passenger connections, w_{ij} are assigned by adjusting the number of passengers connected. Turn back in one way is not allowed for the passenger connections.

In Table 6, we give the airport congestion coefficients used in this experimental study. These coefficients are normalized using the number of passengers visiting the airports, which is obtained from the T-100 market data of BTS (2010b). The most congested airport in the published schedule has 1.96 congestion level and the least congested airport has 0.64.

We estimate the aircraft turnaround time needed for an aircraft at an airport by multiplying the base aircraft turntime with the airport congestion coefficients as in Eq. (45). Therefore, turntime of an aircraft visiting a congested airport is longer. The calculated aircraft turntimes match with the aircraft turntimes given in Arıkan et al. (2012). Moreover, turntime between through flights are taken as 70% of the calculated turntimes, because boarding time of passengers and time to load and unload their cargos require less time.

$$TA_{ij}^{t} = BaseTurntime^{t} \cdot e_{Dn_i} \tag{45}$$

To be consistent with the published schedule, the departure time of the first flight of each path is set to the departure time of the first flight in the published schedule. Time window constraints are imposed upon the rest of the flights.

In this study, we have a bi-criteria problem where the conflicting objectives are maximization of the service level for passenger connections and minimization of airline's overall cost. In Fig. 3, we show the efficient frontier for a single problem instance using a flight schedule with the first 41 flights of the published schedule in Table 4. We set each experimental factor to the highest value. It can be clearly seen that, when airlines try to maximize the service level for passenger connections, their operational cost increases as expected. The sharp increase in the operational cost occurs while ensuring a higher service level than 0.95. On the other hand, the minimum cost is obtained at the lowest service level.

Table 4
Published schedule.

Tail No	Flight no	Departure	Arrival	Departure time	Flight time	Arrival time	Tail no	Flight No	Departure	Arrival	Departure time	Flight time	Arrival time
N531AA	2303	ORD	DFW	6:45	2:35	9:20	N3DMAA	568	ORD	FLL	7:25	2:55	10:20
N531AA	2336	DFW	ORD	10:10	2:30	12:40	N3DMAA	711	FLL	ORD	11:10	3:15	14:25
N531AA	1053	ORD	AUS	13:25	2:50	16:15	N3DMAA	2021	ORD	SJU	15:25	4:35	20:00
N531AA	336	AUS	ORD	17:00	2:45	19:45	N544AA	2463	ORD	MCI	6:25	1:30	7:55
N531AA	336	ORD	LGA	20:40	2:14	22:54	N544AA	754	MCI	ORD	8:40	1:30	10:10
N598AA	1341	ORD	SFO	7:50	4:55	12:45	N544AA	2321	ORD	DFW	11:15	2:35	13:50
N598AA	348	SFO	ORD	13:30	4:25	17:55	N544AA	2356	DFW	ORD	14:40	2:30	17:10
N598AA	1521	ORD	TUS	19:15	3:55	23:10	N544AA	2487	ORD	DEN	17:50	2:45	20:35
N475AA	407	ORD	STL	6:20	1:10	7:30	N3EBAA	1565	ORD	MSP	6:40	1:30	8:10
N475AA	755	STL	ORD	8:35	1:15	9:50	N3EBAA	779	MSP	ORD	9:00	1:25	10:25
N475AA	755	ORD	SAT	10:45	3:00	13:45	N3EBAA	779	ORD	SAN	11:35	4:20	15:55
N475AA	408	SAT	ORD	14:30	2:40	17:10	N3EBAA	1358	SAN	ORD	16:45	3:55	20:40
N475AA	408	ORD	PHL	18:05	2:05	20:10	N3EBAA	1358	ORD	BOS	21:50	2:10	0:00
N3EEAA	876	ORD	BOS	6:35	2:10	8:45	N3ETAA	1704	ORD	EWR	6:35	2:05	8:40
N3EEAA	413	BOS	ORD	9:35	3:05	12:40	N3ETAA	1883	EWR	ORD	9:30	2:40	12:10
N3EEAA	413	ORD	SNA	13:45	4:35	18:20	N3ETAA	810	ORD	DCA	13:10	1:40	14:50
N3EEAA	1262	SNA	ORD	19:10	3:50	23:00	N3ETAA	2013	DCA	ORD	15:45	2:10	17:55
N4YDAA	451	ORD	SFO	9:45	4:55	14:40	N3ETAA	2013	ORD	LAS	19:00	4:05	23:05
N4YDAA	554	SFO	ORD	15:45	4:25	20:10	N3DYAA	1063	ORD	LAX	8:50	4:35	13:25
N3ERAA	496	ORD	DCA	6:45	1:40	8:25	N3DYAA	874	LAX	ORD	14:30	4:15	18:45
N3ERAA	1715	DCA	ORD	9:15	2:10	11:25	N3DYAA	874	ORD	BOS	19:45	2:10	21:55
N3ERAA	1715	ORD	LAS	12:25	4:05	16:30	N5DXAA	1048	ORD	MIA	7:35	3:00	10:35
N3ERAA	1708	LAS	ORD	17:20	3:40	21:00	N5DXAA	1763	MIA	ORD	11:55	3:20	15:15
N5CLAA	1425	ORD	SNA	8:25	4:40	13:05	N5DXAA	1899	ORD	MIA	16:20	3:00	19:20
N5CLAA	556	SNA	ORD	14:00	4:00	18:00	N454AA	2441	ORD	ATL	6:30	2:00	8:30
N5CLAA	1940	ORD	MIA	19:25	3:00	22:25	N454AA	1986	ATL	ORD	9:15	2:15	11:30
N535AA	2460	ORD	RSW	6:45	2:45	9:30	N454AA	1872	ORD	MCO	12:25	2:40	15:05
N535AA	564	RSW	ORD	10:20	3:05	13:25	N454AA	1131	MCO	ORD	15:50	3:05	18:55
N535AA	1446	ORD	EWR	14:55	2:45	17:40	N4YMAA	1137	ORD	MSY	8:20	2:25	10:45
N535AA	1411	EWR	ORD	18:45	2:45	21:30	N4YMAA	1768	MSY	ORD	11:30	2:30	14:00
N3DRAA	1021	ORD	LAS	8:30	4:05	12:35	N4YMAA	1768	ORD	PHL	15:05	2:05	17:10
N3DRAA	1544	LAS	ORD	13:25	3:40	17:05	N4YMAA	1697	PHL	ORD	18:00	2:35	20:35
N3DRAA	1544	ORD	DCA	18:00	1:40	19:40	N420AA	1686	ORD	RDU	6:50	1:50	8:40
N467AA	1823	ORD	PBI	9:20	2:55	12:15	N420AA	2435	RDU	ORD	9:25	2:15	11:40
N467AA	2067	PBI	ORD	13:00	3:20	16:20	N420AA	2435	ORD	PHX	12:35	4:00	16:35
N467AA	2067	ORD	STL	17:15	1:10	18:25	N420AA	1206	PHX	ORD	17:15	3:30	20:45
N467AA	1186	STL	ORD	19:10	1:15	20:25	N546AA	1462	ORD	EWR	8:00	2:45	10:45
N3DTAA	2363	ORD	HDN	9:50	2:50	12:40	N546AA	1387	EWR	ORD	11:25	2:45	14:10
N3DTAA	2318	HDN	ORD	13:40	2:50	16:30	N546AA	1397	ORD	MCO	15:00	2:40	17:40
N412AA	2345	ORD	DFW	17:15	2:35	19:50	N546AA	1221	MCO	ORD	18:25	2:55	21:20
N412AA	2374	DFW	ORD	20:40	2:20	23:00	N4WPAA	2311	ORD	DFW	9:05	2:35	11:40
N530AA	398	ORD	LGA	6:15	2:14	8:29	N4WPAA	2348	DFW	ORD	12:35	2:20	14:55
N530AA	319	LGA	ORD	9:25	2:50	12:15	N4WPAA	1797	ORD	STL	15:50	1:10	17:00

(*continued on next page*)

Table 4 (*continued*)

Tail No	Flight no	Departure	Arrival	Departure time	Flight time	Arrival time	Tail no	Flight No	Departure	Arrival	Departure time	Flight time	Arrival time
N530AA	2329	ORD	DFW	13:35	2:35	16:10	N4WPAA	1982	STL	ORD	18:00	1:15	19:15
N530AA	2364	DFW	ORD	17:00	2:30	19:30	N4WPAA	1339	ORD	SAN	20:15	4:30	0:45
N459AA	394	ORD	LGA	6:50	2:15	9:05	N439AA	2455	ORD	PHX	7:10	4:00	11:10
N459AA	321	LGA	ORD	10:00	2:50	12:50	N439AA	358	PHX	ORD	11:55	3:30	15:25
N459AA	366	ORD	LGA	13:55	2:20	16:15	N439AA	358	ORD	LGA	16:25	2:15	18:40
N459AA	347	LGA	ORD	17:15	2:50	20:05	N439AA	371	LGA	ORD	20:00	2:50	22:50
N4XGAA	2079	ORD	SAN	8:45	4:30	13:15	N5EBAA	2375	ORD	EGE	8:10	2:55	11:05
N4XGAA	1438	SAN	ORD	14:00	4:10	18:10	N4EBAA	2378	EGE	ORD	12:25	2:45	15:10
N4XGAA	346	ORD	LGA	19:50	2:15	22:05	N4EBAA	1677	ORD	SNA	18:40	4:40	23:20
N536AA	2305	ORD	DFW	7:45	2:35	10:20	N3DUAA	2099	ORD	LAX	7:00	4:35	11:35
N536AA	2344	DFW	ORD	11:35	2:30	14:05	N3DUAA	1972	LAX	ORD	12:40	4:15	16:55
N536AA	1201	ORD	STL	14:50	1:05	15:55	N3DUAA	1972	ORD	RDU	17:45	1:55	19:40
N536AA	1815	STL	ORD	17:00	1:20	18:20	N3ELAA	2057	ORD	SJU	8:30	4:35	13:05
N536AA	1815	ORD	SLC	19:15	3:40	22:55	N3ELAA	2078	SJU	ORD	14:25	5:35	20:00

Table 5
Aircraft parameters.

Aircraft type	B727 228	B737 500	MD 83	A320 111	A320 212	B767 300
Capacity	134	122	148	172	180	218
Mass (kgs)	74,000	50,000	61,200	62,000	64,000	135,000
Surface(m^2)	157.9	105.4	118	122.4	122.6	283.3
$C_{D0,\ CR}$	0.018	0.018	0.0211	0.024	0.024	0.021
$C_{D2,\ CR}$	0.06	0.055	0.0468	0.0375	0.0375	0.049
Cf_1	0.53178	0.46	0.7462	0.94	0.94	0.763
Cf_2	276.72	300	638.59	50,000	100,000	1,430
cf_{CR}	0.954	1.079	0.9505	1.095	1.06	1.0347
MRC speed	867.6	859.2	867.6	855.15	868.79	876.70
Base turntime	32	36	26	28	30	40
Idle time cost($)	150	140	142	136	144	147

Table 6
Congestion coefficients (e_b).

Airport	Location	Coefficient	Airport	Location	Coefficient
MIA	Miami, FL	1.96	DCA	Washington, DC	1.17
ORD	Chicago, IL	1.88	SAN	San Diego, CA	1.10
LAX	Los Angeles, CA	1.82	STL	St.Louis, MO	1.10
DEN	Denver,CO	1.82	MCI	Kansas City, MO	1.04
DFW	Dallas, TX	1.74	AUS	Austin, TX	1.00
LGA	New York, NY	1.69	RDU	Raleigh/Durham, NC	1.00
BOS	Boston, MA	1.69	MSY	New Orleans, LA	0.96
ATL	Atlanta, GA	1.64	SNA	Santa Ano, CA	0.96
PHX	Phoenix, AZ	1.56	SAT	San Antonio, TX	0.90
LAS	Las Vegas, NV	1.56	RSW	Fort Myers, FL	0.90
SFO	San Fransisco, CA	1.44	SJU	San Juan, PR	0.85
MSP	Minneapolis, MN	1.32	PBI	West Palm Beach, FL	0.81
PHL	Philadelphia, PA	1.32	TUS	Tuscan, AZ	0.77
EWR	Newark, NJ	1.25	MCO	Orlando, FL	0.72
FLL	Fort Lauderdale, FL	1.25	EGE	Eagle, CO	0.72
SLC	Salt Lake City, UT	1.17	HDN	Hayden, CO	0.64

Table 7
Original aircraft types.

Tail no	Aircraft type	Tail no	Aircraft type
N531AA	B767 300	N5CLAA	B767 300
N598AA	B767 300	N535AA	B767 300
N475AA	A320 212	N3DRAA	A320 111
N3EEAA	A320 111	N467AA	A320 212
N4YDAA	A320 212	N3DTAA	A320 111
N3ERAA	A320 111	N412AA	A320 212

5.1. Analysis on the schedule with 41 flights

In this experimental study, we use a flight schedule which is generated by taking the first 41 flights of the published schedule in Table 4. We consider 12 different aircraft with 3 different types and randomly assign aircraft types in Table 7.

We first test the performance of the schedule achieved by the integrated model with the published schedule. Afterwards, we compare the results of the two-stage algorithm and the optimal solutions of the integrated model.

5.1.1. Computational analysis on the integrated model

We give a comparison among different cost components between the integrated model's optimum solution and published schedule in Table 8. We summarize the results for 40 problem instances. For each factor level, we report the minimum, average and maximum reduction in fuel and emission costs, idle time cost, total cost and total cost without considering delay over five replications. We consider delay cost of the published schedule, when we calculate the total cost improvement. Unit delay cost is difficult to determine. To simplify the calculation, we assume a linear delay cost with $200 per minute of delay. But, it is evident that integrated model performs better cost savings in total cost even without including the delay cost. The improvement percentages are calculated using the following formula:

$$\text{Cost Improvement (\%)} = 100 \times \frac{\text{Published Schedule - Integrated Model}}{\text{Published Schedule}}$$

The effect of the fuel price per ton has a significant impact on the total cost improvement. The integrated model has much more tendency to decrease fuel consumption, when fuel price is high. Therefore, integrated model assigns the fuel efficient aircraft to the paths which require more fuel consumption and adjusts the speed of the aircraft to minimize the fuel consumption. As a result, fuel and CO_2 emission cost improvements increase. On the other hand, the cost of the spilled passengers increases with this assignment so that it leads to low total cost improvements.

When base spill cost is high, this leads to much more demand satisfaction to reduce the cost of spilled passengers. However, this approach incurs higher fuel and CO_2 emission costs which constitute the major portion of the airline operational costs. Therefore, total cost saving decreases compared to the low setting.

β scale parameter of the log-Laplace distribution has significant effects on the idle time and total cost improvements. It is observed that our model achieves better idle time and total cost savings when β is low, and the performance of the model in improving fuel and emission costs is slightly affected by β. The reason behind this is that a higher β causes a higher variance in non-cruise times of flights, which necessitates more idle time insertion and compression on the cruise times to ensure the connections. Therefore, this leads to more idle time and total operational costs.

Overall, improvements in the cost of fuel and CO_2 emissions are approximately 11%, whereas the improvement in idle time is approximately 68%. However, 2% of the passengers are not satisfied due to limited seat capacity of the aircraft. It is observed that

Table 8
Comparison of factor effects.

		Fuel & emis. cost improvement			Idle cost improvement			Total cost improvement			Total impr. without delay		
		Min	Avg	Max	Min	Avg	Max.	Min	Avg	Max	Min	Avg.	Max
C_{fuel} ($/kg)	Low	8.3	11.1	12.3	59.8	68.4	79.8	20.5	24.5	29.2	18.2	23.3	28.8
	High	10.5	11.7	12.3	59.4	68.1	79.8	16.6	19.3	22.4	15.2	18.5	22.2
Base Spill Cost	Low	12.1	12.3	12.3	59.5	67.9	79.8	19.2	23.1	29.2	17.8	22.1	28.8
	High	8.3	10.5	12.3	59.4	68.5	79.8	16.6	20.7	27.3	15.2	19.6	26.9
β	Low	8.9	11.6	12.3	69.2	75.5	79.8	17.5	23.2	29.2	17.2	22.8	28.8
	High	8.3	11.1	12.3	59.4	61.0	66.3	16.6	20.7	24.9	15.2	18.9	22.7

Table 9
Cost comparison for different replications.

	Fuel & emis. cost improvement (%)			Idle cost improvement (%)			Total cost improvement (%)		
Replications	Min	Avg	Max	Min	Avg	Max.	Min	Avg	Max
1	8.3	11.1	12.3	59.6	68.3	77.1	16.7	21.7	27.5
2	8.9	11.1	12.3	59.4	67.9	76.3	16.6	21.5	27.1
3	11.1	11.9	12.3	60.1	69.7	79.8	18.6	23.3	29.2
4	9.0	11.6	12.3	61.7	65.9	70.2	16.7	20.8	25.8
5	8.8	11.2	12.3	61.0	69.3	76.5	17.6	22.3	27.5

Table 10
CPU time analysis of the integrated model.

		CPU time (sec)		
Factor	Level	Min	Avg	Max
C_{fuel} ($/kg)	Low	758	2250	6490
	High	606	3425	11290
Base Spill Cost	Low	606	3474	11290
	High	743	2201	6490
β	Low	606	2350	7303
	High	743	3325	11290

the fuel and CO_2 emission cost savings compensate the cost of the spilled passengers, thus resulting in 22% total cost improvement.

We take five replications for each factor combination to observe if random values of passenger demand and passenger connection times have any impact on objective values. For each replication, the minimum, average and maximum improvements in each cost component are seen in Table 9. We could conclude that there is no statistically significant randomization effect on the objective function values.

To see the effect of each factor on the computation time, minimum, average and maximum values of CPU in seconds over five replications are analyzed in Table 10. Increase in fuel price makes aircraft-path assignment decisions more crucial. As expected this requires much more CPU time to deal with the nonlinear fuel and emission cost functions. If the base spill cost increases, then the seat capacity of the aircraft becomes more significant on the fleet assignment strategy. The problem complexity decreases, thereby decreases the overall computation time. Increasing the variability, i.e., β, increases the problem complexity as it becomes harder to satisfy the connections at a desired service level. As a result, the required CPU time increases.

Moreover the average CPU time requirement for solving the mixed integer second order conic formulation is 3000 CPU seconds. As expected, the conflicting objectives increase the problem complexity and the computation time. When the fuel price and β parameters are high and base spill cost is low, maximum time to solve the five problem instances reaches to 11,290 CPU seconds. Therefore, we also devise a two-stage algorithm to solve the large scale problems in a reasonable time.

5.1.2. Computational analysis on the two-Stage algorithm

In this section, we use the same generated schedule having 41 flights operated by 12 different aircraft with 3 different types. We similarly perform a 2^3 full-factorial experimental design with 5 replications. The parameter, m, to generate m schedules in the two-stage algorithm is set to three and the length of the tabu list is taken as 1. In order to test the solution quality of the two-stage algorithm, we compare the total cost of the schedule generated by the two-stage algorithm with the optimum solution of the integrated model. Optimality gap for the two-stage algorithm is calculated as the following:

$$\text{Optimality gap} = \frac{\text{Two-Stage Algorithm - Integrated Model}}{\text{Integrated Model}}$$

For each factor combination, we provide the average optimality gap over 5 replications in Table 11. When the factors C_{fuel} , Base Spill Cost and β are set to their low, high and high values, total cost of the schedule developed by the two-stage algorithm is approximately 0.001 times worse than the total cost of the schedule achieved by the integrated model as well as the high, high and low setting, respectively. For the remaining ones, achieved costs by the two-stage algorithm are approximately the same as the optimal solutions of the integrated model.

In addition, for only 6 instances out of 40 the instances, the fleet type assignment obtained by the two-stage algorithm differs from the optimal solutions of the integrated model. The gaps between the objectives are negligible for these instances. Our computational results indicate that for the reasonable size of the problem, the two-stage algorithm gives very similar results to the optimum solutions in seconds.

5.2. Analysis on the schedule with 114 flights

For this computational study, we utilize the published schedule in Table 4. The schedule has 114 flights operated by 32 different aircraft with six different types. We again perform a 2^3 full-factorial experimental design with 5 replications. We first solve the mixed integer second order conic programming formulation within a time limit of 9000 CPU seconds. We obtain the best known upper bound (objective) and the best lower bound (LB) at the time of the termination. Then, we also run the two-stage algorithm. We calculate the relative gap between the LB obtained by the integrated

Table 11
Gap between two-stage algorithm and the integrated model.

Factor			Optimality	Factor			Optimality
C_{fuel} ($/kg)	Base Spill Cost	β	Gap	C_{fuel} ($/kg)	Base Spill Cost	β	Gap
Low	Low	Low	0.000	High	Low	Low	0.000
Low	Low	High	0.000	High	Low	High	0.000
Low	High	Low	0.000	High	High	Low	0.001
Low	High	High	0.001	High	High	High	0.000

Table 12
Factor effects on the Gap.

		Gap with LB (%) for integrated model			Gap with LB (%) for two-stage alg.		
Factor	Level	Min	Avg	Max	Min	Avg	Max
C_{fuel} ($/kg)	Low	5.4	7.1	10.5	2.2	6.0	7.7
	High	4.9	7.8	10.0	2.6	6.3	8.1
Base Spill Cost	Low	5.9	8.6	10.5	4.0	7.1	8.1
	High	4.9	6.2	7.7	2.2	5.1	6.1
β	Low	4.9	7.2	10.5	2.2	5.7	8.0
	High	5.4	7.7	10.0	5.0	6.6	8.1

Table 13
Factor effects on relative performance.

		Relative performance (%)		
Factor	Level	Min	Avg	Max
C_{fuel} ($/kg)	Low	0.1	−1.0	−4.9
	High	−0.8	−1.3	−3.0
Base Spill Cost	Low	−0.3	−1.4	−4.9
	High	0.1	−1.0	−3.0
β	Low	−0.3	−1.3	−4.9
	High	0.1	−1.0	−3.0

model within the time limit and the objective of the two-stage algorithm. In a similar way, we also calculate the relative gap with the LB for the integrated model. We give the calculations of relative gaps with the LB as follows:

$$\text{Gap with LB for Two-stage Alg. (\%)} = 100 \times \frac{\text{Objective of Two-stage Alg. - LB}}{\text{LB}}$$

$$\text{Gap with LB for Integrated Model (\%)} = 100 \times \frac{\text{Objective of Integrated Model - LB}}{\text{LB}}$$

Table 12 illustrates the minimum, average and maximum of the relative gaps over five replications both for the integrated model and the two-stage algorithm. On the average, the gap with lower bound for the integrated model is 7.43%, whereas it is 6.14% for the two-stage algorithm. It is important to clarify that, on the average, the gap for the two-stage algorithm is less than the integrated model within the time limit of 9000 CPU seconds. In other words, on the average, the two-stage algorithm results in a lower cost schedule than the best incumbent solution found by the integrated model within given time limit.

Moreover, for 18 instances out of the 40 instances, the relative gap for the two-stage algorithm becomes less than 6%, whereas 6 of them result in 5% gap. However, we do not know whether the lower bound is weak or strong. Thus, the optimality gap with the lower bound is not enough to analyze the performance of two-stage algorithm. We also compare the results of the two-stage algorithm to the best incumbent solutions found by the integrated model within 9000 CPU seconds as follows:

$$\text{Relative Performance (\%)} = 100 \times \frac{\text{Objective of Two-stage Alg. - Objective of IM}}{\text{Objective of IM}}$$

Integrated model could not reach optimal solutions within the time limit of 9000 CPU seconds. Even, for 39 out of 40 instances, solutions of two-stage approach give lower cost than the best incumbent solutions of the integrated model. In Table 13, negative values represent a better performance for two-stage approach compared to solutions of the integrated model within the time limit. For instance, when fuel price is low, two-stage approach obtains a maximum cost saving of 4.9% relative to the best incumbent solution. On the average of 40 instances, two-stage algorithm gives 1.18% total cost saving compared to the best solutions found by the integrated model. For 20 out of 40 instances, two-stage algorithm provides 1% cost saving, where 4 of them results in 2% cost saving. On the other hand, for only 1 instance over 40 instances, two-stage algorithm gives 0.1% higher cost than the best solution of the integrated model, when factors C_{fuel}, Base Spill Cost and β are at their low, high and high levels, respectively. We can conclude that two-stage approach is capable of producing very promising results compared to the best solutions of the integrated model within 9000 CPU seconds.

We also provide different cost improvements for two-stage approach compared to the published schedule in Table 14. It can be seen that, the results of the two-stage algorithm are very promising as well. Idle time cost savings are approximately 70%, whereas the fuel and emission cost reductions are approximately 4.5%. The overall cost saving is around 21%. These are similar to the analysis on the schedule with 41 flights.

Our computational results indicate that fuel and CO_2 emission cost improvements increase as the fuel price increases. In contrast, percentage of the spilled passengers increases as it is seen in Table 15. Total cost saving decreases together with increase in the cost of spilled passengers and slightly decrease in idle time cost improvement.

Table 15 also illustrates that high value of the base spill cost decreases the number of spilled passengers, as expected. However, this decreases the fuel and CO_2 emission cost improvements, thereby resulting in lower total cost savings.

In Table 15, we clearly observe the impact of flight time uncertainty on the passenger spill. Table 14 shows that increase in the variability decreases the idle time cost improvements as well as fuel and carbon emission cost improvements. The reason behind this is that our approach inserts larger idle times over critical connections and compresses the cruise time of flights to ensure the passenger connections with a higher service level. At this point, making the appropriate fleet assignment decisions through the network based on the availabilities, seat capacities and demand forecasts becomes more crucial to decrease the operational expenses. It may be preferable to assign a fuel efficient but a smaller aircraft to a certain flight path involving critical passenger connections in albeit of an additional cost of spilled passengers. As it is seen in Table 15, increase in the variability results in more number of spilled passengers as expected.

Table 14
Comparison of factor effects.

		Fuel & emis. cost improvement			Idle cost improvement			Total cost improvement			Total impr. without delay		
		Min	Avg	Max	Min	Avg	Max.	Min	Avg	Max	Min	Avg.	Max
C_{fuel} ($/kg)	Low	2.1	3.7	4.9	69.4	72.5	78.4	23.3	25.2	28.0	20.1	23.0	26.7
	High	4.3	5.3	6.1	68.2	71.6	77.3	16.1	17.6	19.5	14.2	16.2	18.7
Base Spill Cost	Low	4.4	5.3	6.1	68.7	72.3	78.4	18.0	22.3	29.0	15.9	20.5	26.7
	High	2.1	3.7	4.8	68.2	71.9	77.6	16.1	20.6	25.9	14.2	18.7	24.7
β	Low	2.4	4.6	6.1	68.2	72.5	78.4	16.1	21.8	28.0	15.2	20.7	26.7
	High	2.1	4.4	6.1	69.2	71.7	75.8	16.3	21.1	26.6	14.2	18.5	23.5

Table 15
Factor effects on the percentage of spilled passengers.

		Spilled passengers (%)		
Factor	Level	Min	Avg	Max
C_{fuel} ($/kg)	Low	0.5	1.3	2.3
	High	1.0	2.2	3.7
Base Spill Cost	Low	1.4	2.4	3.7
	High	0.5	1.0	1.5
β	Low	0.5	1.7	3.4
	High	0.5	1.8	3.7

Table 16
CPU time analysis of two-stage algorithm.

		CPU time (sec)		
Factor	Level	Min	Avg	Max
C_{fuel} ($/kg)	Low	52	140	269
	High	48	113	187
Base Spill Cost	Low	48	137	269
	High	52	117	214
β	Low	48	93	158
	High	80	160	269

Another measure of interest is the service level of the passengers' connections. For the accuracy of the performance of the generated schedule, the overall desired service level (γ) for passenger connections is taken as equal to the overall service level of the published schedule. In the published schedule, for the lower case of β, the service level is 0.99, whereas it is 0.96 for the higher case. These values are highly satisfactory to ensure the passenger connections with high probabilities.

Table 16 summarizes the CPU time requirement to achieve these results for the two-stage algorithm. As expected, the value of β increases the problem complexity as the increase in the variability. The fuel cost and base spill cost parameters have slightly less effects on the computation time. To solve the larger problem instances with 114 flights, maximum CPU time spent for the two-stage algorithm is 120 s, which is still reasonable to generate a robust schedule in real time.

5.3. Analysis on the schedule with 400 flights

In our previous results, it can be seen that two-stage algorithm provides very promising results on the schedule with 114 flights operated by 32 different aircraft. In order to demonstrate the actual performance of the algorithmic approach on a more realistic network, we construct another sample schedule which has 400 flights operated by 119 different aircraft, almost quadruple the size of the previous schedule in terms of the number of flights and the number of aircraft. The new flight schedule is also constructed by selecting 400 flights from the work of Arıkan et al. (2016) which was extracted from the database "Airline On-Time Performance Data" provided by the Bureau of Transportation Statistics of the US Department of Transportation, BTS (2010a).

Although we show that there is no statistically significant randomization effect on the objective function values, for each experimental setting, we still generate five replications. We summarize the results for 40 problems solved by the two-stage algorithm in Table 17.

Table 17 compares the performance of the schedule generated by the two-stage algorithm and the published schedule. It can be seen that results are very promising for relatively larger size of the problems as well. The overall cost saving is approximately 24%, whereas the reduction in idle time cost and fuel and emission costs are around 78% and 9%, respectively. These are very similar to our previous results. Although the performance of the two-stage algorithm is not affected by the size of the data, the fuel and emission cost savings could be affected by the number of aircraft for each type used in the published schedule.

Moreover, the average CPU time that the two-stage algorithm requires to achieve these results is approximately 6500 s. Maximum amount of time spent is around 13,300 s. It is important to note that these CPU time requirements are reasonable for successful implementation of such a decision making approach in real time.

6. Conclusions

We develop a global optimization tool to simultaneously retime the flight departures and assign aircraft types to paths in a given time period. We capture the flight time uncertainty through the chance constraints to ensure passenger connections. In order to increase the passenger connection opportunities, we slightly allow changes in departure times and adjust the speed of the aircraft in response to flight time uncertainty. The crucial contribution of this paper is to consider the fuel burn and CO_2 emissions costs associated with adjusting cruise speed to ensure the passenger connections. Therefore, one may prefer to assign a fuel efficient but smaller aircraft to a flight path with critical passenger connections in albeit of an additional cost of spilled passengers. In order to handle the nonlinear costs and chance constraints, we use the conic quadratic programming and obtain the exact solutions as opposed to the approximation methods. We also develop a two-stage algorithm which decomposes the problem into two stages such as aircraft-path assignment and robust airline scheduling, and then solves them sequentially. Computational experiments indicate that the two-stage algorithm performs high quality results in acceptable times.

There are several research directions arising from this work that could be pursued. Great advantages of conic structure of the proposed model enable researchers to integrate more planning stages of airline operations. The current model takes the aircraft paths as input and assigns the aircraft types to these paths. One of the integrations would be to determine the assignment of fleet types to the flight legs without knowing the aircraft path priori. The prob-

Table 17
Comparison of factor effects of the schedule with 400 Flights.

		Fuel & emis. cost improvement (%)			Idle cost improvement (%)			Total cost improvement (%)		
		Min	Avg	Max	Min	Avg	Max.	Min	Avg	Max
C_{fuel} ($/kg)	Low	5.5	8.1	10.3	77.5	80.0	82.7	26.1	27.8	29.6
	High	9.0	10.2	11.3	73.7	76.5	79.6	19.0	20.6	22.2
Base Spill Cost	Low	9.8	10.6	11.3	75.3	78.5	81.6	21.7	25.5	29.6
	High	5.5	7.7	9.6	73.7	78.2	82.7	18.9	22.9	27.0
β	Low	5.6	9.2	11.3	73.7	77.7	81.0	19.3	24.4	29.6
	High	5.5	9.1	11.2	75.2	78.9	82.7	18.9	24.0	29.2

lem can be further extended to involve the crew assignment decisions as well as the fleet assignment decisions.

One such direction would be to capture the variability in non-cruise times by using stochastic programming. The current method models the variability with chance constraints to ensure the desired service level for passenger connections. The uncertainty would be also handled by a stochastic model where many of potential delay scenarios are analyzed. The effect on delay propagation could be conducted in the enlarged problem involving aircraft, passenger and crew connections through the entire network. On the other hand, considering many scenarios may lead to large decision trees that could requires significant computation time to solve the overall stochastic model.

Appendix A

A1. Log-Laplace distribution

The probability density and cumulative distribution functions of Log-Laplace random variable A_i with a scale parameter, e^{α} and the tail parameter, $1/\beta_i$ are

$$f_{A_i}(x) = \begin{cases} \frac{1}{2\cdot\beta_i\cdot x} e^{\frac{(\ln(x)-\alpha)}{\beta_i}}, & \text{if } \ln(x) < \alpha \\ \frac{1}{2\cdot\beta_i\cdot x} e^{\frac{-(\ln(x)-\alpha)}{\beta_i}}, & \text{if } \ln(x) \geq \alpha \end{cases}$$

$$F_{A_i}(x) = \begin{cases} \frac{1}{2} e^{\frac{(\ln(x)-\alpha)}{\beta_i}}, & \text{if } \ln(x) < \alpha \\ 1 - \frac{1}{2} e^{\frac{-(\ln(x)-\alpha)}{\beta_i}}, & \text{if } \ln(x) \geq \alpha \end{cases}$$

The quantile function of the random variable A_i, which will be used in transformation of the chance constraints into the second order conic inequalities, is given as:

$$F^{-1}_{A_i}(p) = \begin{cases} (2p)^{\beta_i}\cdot e^{\alpha}, & \text{if } p < \frac{1}{2} \\ \frac{e^{\alpha}}{(2-2p)^{\beta_i}}, & \text{if } p \geq \frac{1}{2} \end{cases}$$

A2. Fuel cost function

To estimate the fuel burn, we used the cruise stage fuel flow model developed by the Base of Aircraft Data (BADA) (EUROCONTROL, 2012). Then, for a given mass of the aircraft and fuel consumption coefficients, fuel burn rate (kg/min) as a function of the speed V (km/min) can be calculated as:

$$f_{cr}(V) = \frac{1}{2}\cdot C_{f1}\cdot C_{fcr}\cdot\left(C_{D0,CR}\cdot\rho\cdot S\cdot V^2 + C_{D0,CR}\cdot\frac{\rho\cdot S}{C_{f2}}V^3 + C_{D2,CR}\cdot\frac{4\cdot m^2\cdot g_0^2}{\rho\cdot S\cdot\cos(\phi)^2\cdot V^2} + C_{D2,CR}\cdot\frac{4\cdot m^2\cdot g_0^2}{C_{f2}\cdot\rho\cdot S\cdot\cos(\phi)^2\cdot V}\right) \quad (46)$$

where aircraft specific fuel consumption coefficients, C_{f1}, C_{f2}, C_{fcr}, $C_{D0,\,CR}$ and $C_{D2,\,CR}$, wing surface area, S, and mass of the aircraft, m, are taken from EUROCONTROL (2012) and listed in Table 5. ρ, g_0 and ϕ are the air density (kg/m^3) at given altitude, gravitational acceleration (m/s^2) and bank angle, respectively. We assume that the distance flown at cruise stage is fixed d, and hence the cruise duration is expressed as d/V. We can formulate the total fuel consumed (kg) as follows:

$$\begin{aligned} F(V) &= \frac{d}{V}\cdot f_{cr}(V) \\ &= \frac{1}{2}\cdot d\cdot C_{f1}\cdot C_{fcr}\cdot \left(C_{D0,CR}\cdot\rho\cdot S\cdot V + C_{D0,CR}\cdot\frac{\rho\cdot S}{C_{f2}}V^2 \right. \\ &\quad + C_{D2,CR}\cdot\frac{4\cdot m^2\cdot g_0^2}{\rho\cdot S\cdot\cos(\phi)^2\cdot V^3} \\ &\quad \left. + C_{D2,CR}\cdot\frac{4\cdot m^2\cdot g_0^2}{C_{f2}\cdot\rho\cdot S\cdot\cos(\phi)^2\cdot V^2}\right) \end{aligned} \quad (47)$$

We can rewrite the fuel consumption in terms of the cruise time by replacing V by $\frac{d_i}{f_i^t}$ for each flight $i \in J$ and aircraft $t \in T$. Then, total fuel consumed as a function of cruise time can be expressed as:

$$F_i^t\left(f_i^t\right) = c_1^{i,t}\cdot\frac{1}{f_i^t} + c_2^{i,t}\cdot\frac{1}{\left(f_i^t\right)^2} + c_3^{i,t}\cdot\left(f_i^t\right)^3 + c_4^{i,t}\cdot\left(f_i^t\right)^2 \quad (48)$$

where

$$c_1^{i,t} = \frac{1}{2}\cdot C_{f1}^t\cdot C_{fcr}^t\cdot C_{D0,CR}^t\cdot\rho\cdot S^t\cdot d_i^2$$

$$c_2^{i,t} = \frac{1}{2}\cdot C_{f1}^t\cdot C_{fcr}^t\cdot\frac{C_{D0,CR}^t\cdot\rho\cdot S^t\cdot d_i^3}{C_{f2}^t}$$

$$c_3^{i,t} = \frac{1}{2}\cdot C_{f1}^t\cdot C_{fcr}^t\cdot\frac{C_{D2,CR}^t\cdot 4\cdot m_t^2\cdot g_0^2}{\rho\cdot S^t\cdot\cos(\phi)^2\cdot d_i^2}$$

$$c_4^{i,t} = \frac{1}{2}\cdot C_{f1}^t\cdot C_{fcr}^t\cdot\frac{C_{D2,CR}^t\cdot 4\cdot m_t^2\cdot g_0^2}{C_{f2}^t\cdot\rho\cdot S^t\cdot\cos(\phi)^2\cdot d_i^2}$$

References

Ahmadbeygi, S., Cohn, A., Lapp, M., 2010. Decreasing airline delay propagation by re-allocating scheduled slack. IIE Trans. 42, 478–489.

Aktürk, M.S., Atamtürk, A., Gürel, S., 2014. Aircraft rescheduling with cruise speed control. Oper. Res. 62, 829–845.

Arıkan, M., Deshpande, V., 2012. The impact of airline flight schedules on flight delays. Manuf Serv. Oper. Manage 14 (3), 423–440.

Arıkan, M., Deshpande, V., Sohoni, M., 2012. Building reliable air-travel infrastructure using empirical data and stochastic models of airline networks. Oper. Res. 61 (1), 45–64.

Arıkan, U., Gürel, S., Aktürk, M.S., 2016. Integrated aircraft and passenger recovery with cruise time controllability. Ann. Oper. Res. 236 (2), 295–317.

Ben-Tal, A., Nemirovski, A., 2001. Lectures on modern convex optimization: Analysis, algorithms, and engineering applications. SIAM.

Bertsimas, D., Lulli, G., Odoni, A., 2010. An integer optimization approach to large-scale air traffic flow management. Oper. Res. 59, 211–227.

Boeing,. Airplane characteristics for airport planning. http://www.boeing.com/commercial/airports/plan_manuals.page. Visited June 2014.

BTS, 2010a. Airline on-time performance dataVisited May 2014.

BTS, 2010b. T-100 market dataVisited May 2014.

Burke, E.K., De Causmaecker, P., De Maare, G., Mulder, J., Paelinck, M., Vanden Berghe, G., 2010. A multi-objective approach for robust airline scheduling. Comput. Oper. Res. 37, 822–832.
Chiraphadhanakul, V., Barnhart, C., 2013. Robust flight schedules through slack re-allocation. EURO J.Transp. Logist. 2, 277–306.
Cook, A., Tanner, G., Williams, G., Meise, G., 2009. Dynamic cost indexing-managing airline delay costs. J. Air Transp. Manage. 15, 26–35.
Dunbar, M., Froyland, G., Wu, C.L., 2014. An integrated scenario-based approach for robust aircraft routing, crew pairing and re-timing. Comput. Oper. Res. 45, 68–86.
Duran, A.S., Gürel, S., Aktürk, M.S., 2015. Robust airline scheduling with controllable cruise times and chance constraints. IIE Trans. 47 (1), 64–83.
EUROCONTROL, 2001. Forecasting civil aviation fuel burn and emissions in Europe. Technical Report 2001-8. EEC Technical/Scientific, Eurocontrol, Eurocontrol Experimental Centre, B.P. 15, F-91222 Bretigny-sur-Orge, France.
EUROCONTROL, 2012. User manual for the base of aircraft data (BADA) revision 3.10.. Technical Report 12/04/10-45. EEC Technical/Scientific, Eurocontrol, Eurocontrol Experimental Centre, B.P. 15, F-91222 Bretigny-sur-Orge, France.
Günlük, O., Linderoth, J., 2010. Perspective reformulations of mixed integer nonlinear programs with indicator variables. Math Program 124, 183–205.
Hai, J., Barnhart, C., 2013. Robust airline schedule design in a dynamic scheduling environment. Comput. Oper. Res. 40, 831–840.
Hiriart-Urruty, J.B., Lemaréchal, C., 2001. Fundamentals of Convex Analysis. Springer, Berlin.
IATA, 2013. Climate change. http://www.iata.org/policy/environment/Pages/climate-change.aspx. Visited February 2016.
IATA, 2014. Fuel price analysis. http://www.iata.org/publications/economics/fuel-monitor/Pages/price-analysis.aspx. Visited May 2014.
ICAO, 2009. ICAO fuel factor. Technical Report. International Civil Aviation Organization (ICAO).
Jarrah, A.I., Goodstein, J., Narasimhan, R., 2000. An efficient airline re-fleeting model for the incremental modification of planned fleet assignments. Transp. Sci. 34 (4), 349–363.
Lan, S., Clarke, J.P., Barnhart, C., 2006. Planning for robust airline operations: optimizing aircraft routings and flight departure times to minimize passenger disruptions. Transp. Sci. 40 (1), 15–28.
Maher, S.J., 2015. A novel passenger recovery approach for the integrated airline recovery problem. Comput. Oper. Res. 57, 123–137.
Marais, K., Waitz, I.A., 2009. Chapter 14 air transport and the environment. In: Belobaba, P., Odoni, A., Barnhart, C. (Eds.), The Global Airline Industry. Wiley, UK, pp. 405–440.
Mercier, A., Soumis, F., 2007. An integrated aircraft routing, crew scheduling and flight retiming model. Comput. Oper. Res. 34, 2251–2265.
Papadakos, N., 2009. Integrated airline scheduling. Comput. Oper. Res. 36 (1), 176–195.
Rexing, B., Barnhart, C., Kniker, T., Jarrah, A., Krishnamurthy, N., 2000. Airline fleet assignment with time windows. Transp. Sci. 34 (1), 1–20.
Sherali, H.D., Bae, K.H., Haouari, M., 2013. A benders decomposition approach for an integrated airline schedule design and fleet assignment problem with flight retiming, schedule balance, and demand recapture. Ann. Oper. Res. 210, 213–244.
Sherali, H.D., Bish, E.K., Zhu, X., 2005. Polyhedral analysis and algorithms for a demand-driven refleeting model for aircraft assignment. Transp. Sci. 39 (3), 349–366.
Sherali, H.D., Staats, R.W., Trani, A.A., 2006. An airspace-planning and collaborative decision-making model: part II-cost model, data considerations, and computations. Transp. Sci. 40, 147–164.
Sherali, H.D., Zhu, X., 2008. Two-stage fleet assignment model considering stochastic passenger demands. Oper. Res. 56 (2), 383–399.
Sohoni, M., Lee, Y., Klabjan, D., 2011. Robust airline scheduling under block time uncertainty. Transp. Sci. 45, 451–464.
Tetzloff, I., Crossley, W., 2010. Impact of future generation aircraft on fleet-level environmental emission metrics. AIAA Paper 9205.
T'kindt, V., Billaut, J.C., 2006. Multicriteria scheduling: Theory, models and algorithms, 2 Springer, Berlin.
Weide, O., Ryan, D., Ehrgott, M., 2010. An iterative approach to robust and integrated aircraft routing and crew scheduling. Comput. Oper. Res. 37, 833–844.